ELSEVIER

Journal of South American Earth Sciences 23 (2007) 122–146

Journal of
South American
Earth Sciences

www.elsevier.com/locate/jsames

Cenozoic subsurface stratigraphy and structure of the Salar de Atacama Basin, northern Chile

T.E. Jordan [a,*], C. Mpodozis [b,c], N. Muñoz [b], N. Blanco [c], P. Pananont [a], M. Gardeweg [c,d]

[a] *Earth and Atmospheric Sciences, Snee Hall, Cornell University, Ithaca, NY 14853-1504, USA*
[b] *SIPETROL S.A., Vitacura 2736, Santiago, Chile*
[c] *SERNAGEOMIN, Avenida Santa Maria 0104, Santiago, Chile*
[d] *Rayén 6740, Vitacura, Santiago, Chile*

Received 1 January 2004; accepted 1 August 2006

Abstract

Sequence mapping of industry seismic lines and their correlation to exposed stratigraphic formations enable a description of the evolution of the nonmarine Salar de Atacama Basin. This major tectonic basin, located in the present-day forearc of the northern Chilean Andes, was first defined topographically by late Cretaceous inversion of the Jurassic–early Cretaceous extensional Tarapacá backarc Basin. Inversion led to both the uplift of the Cordillera de Domeyko and subsidence of the Salar de Atacama Basin along its eastern flank. The basin evolved from a continental backarc in the Cretaceous and Paleogene to a forearc tectonic setting during the Neogene. The principal causes of basin-scale tectonic subsidence include late Cretaceous and earliest Paleocene shortening and Oligocene–early Miocene localized extension. The basin was not completely filled by late Cretaceous (Purilactis Group, sequence G) and Paleocene (sequence H) strata, and its empty space persisted through the Cenozoic. Eocene deformation caused long-wavelength rotation of a deeply weathered surface, generating an erosional unconformity across which coarse clastic strata accumulated (sequence J). Oligocene–early Miocene normal faulting, perhaps in a transtensional environment, repositioned the western basin margin and localized hangingwall subsidence, leading to the accumulation of thousands of meters of evaporitic strata (sequence K, Paciencia Group). By the close of the early Miocene, shortening resumed, first uplifting the intrabasinal Cordillera de la Sal and later generating Pliocene blind reverse faults within the topographically lowest part of the basin. Unequal deposition and tilting across the nascent Cordillera de la Sal induced diapirism of the Paciencia Group halite. In combination, inherited accommodation space and new tectonic subsidence, plus local salt-withdrawal subsidence, shaped the distribution of Upper Miocene–Recent ignimbrites, evaporites, and clastics (sequence M and Vilama Formation).

Keywords: South America; Andes; Forearc; Tectonics; Basin evolution; Cenozoic

1. Introduction

The Salar de Atacama Basin offers an excellent view of the progression of Cenozoic tectonic changes in the region that is now the northern Chilean forearc. In this sedimentary basin, a thick succession of nonmarine strata, whose ages have been established by dating of interbedded volcanic horizons, paleomagnetic studies, and regional correlations, crops out. These strata are characterized by complex facies and thickness changes that include a sensitive record of drainage basin evolution, relative uplift at the margins of the basin, and subsidence. Hooper and Flint (1987), Flint et al. (1993), Jolley et al. (1990), Wilkes and Görler (1994), Kape (1996), Arriagada (1999), Arriagada et al. (2000), Blanco et al. (2000), and Mpodozis et al. (2000, 2005) have contributed to our understanding of the evolution of the Salar de Atacama Basin through studies of rock exposures on the west flank of the basin in the Cerros de Purilactis, Cuesta de Barros Arana, and El Bordo Escarpment (all of which form the eastern border of the Cordillera Domeyko) and the Cordillera de la Sal (Figs. 1 and 2). However, evaluations of basin history, derived largely from the elongate outcrop belt, are

* Corresponding author. Tel.: +1 607 255 3596; fax: +1 607 254 4780.
E-mail address: tej1@cornell.edu (T.E. Jordan).

0895-9811/$ - see front matter © 2006 Elsevier Ltd. All rights reserved.
doi:10.1016/j.jsames.2006.09.024

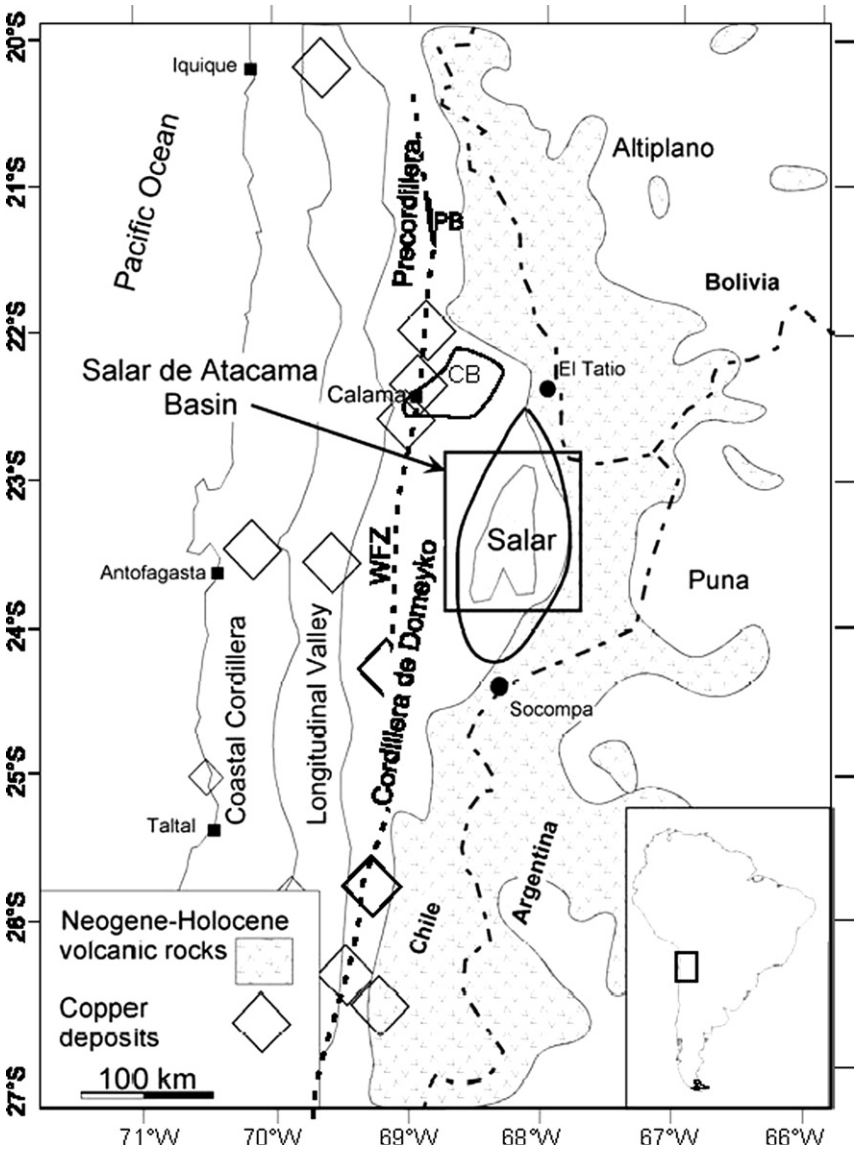

Fig. 1. Regional location map for Salar de Atacama Basin in northern Chile; inset map shows location of regional map relative to South America. The Western Cordillera encompasses most of the area of middle Miocene–Recent volcanic rocks, except the major fingers and patches of volcanic cover that extend eastward. The general position of the Eocene–early Oligocene magmatic arc is represented by the locations of major porphyry copper deposits. The Salar de Atacama Basin was in a backarc position relative to the Paleogene arcs, whose influence spanned the Central Depression to Precordillera (Cordillera de Domeyko) and in a forearc position relative to the Neogene arc. Box shows the area of Fig. 2. Closed region labeled "CB" is the Calama Basin; "PB" is Papajoy Basin; "WFZ" is the West Fissure Fault zone, which moved in a sinistral sense during the Oligocene–early Miocene.

dimensionally limited and can be expanded by the use of an extensive grid of seismic reflection profiles, whose study was pioneered by Macellari et al. (1991), Jordan et al. (2002a,b), Muñoz et al. (1997, 2000, 2002), and, most recently, Arriagada (2003) and Pananont et al. (2004). With these subsurface data plus recent advances in geochronologic age constraints of the strata, we may treat basin evolution comprehensively.

Multiple, conflicting models of the tectonic evolution of the Salar de Atacama Basin have been published. For example, Flint et al. (1993) propose that the Salar de Atacama Basin evolved under extensional tectonic conditions throughout the entire Mesozoic and Cenozoic periods. Muñoz et al. (1997) propose that the basin began as a Cretaceous extensional basin that was subsequently inverted by east-directed thrusting during the late Cretaceous, with compressional or neutral conditions persisting during subsequent intervals of basin fill. Most recently, Arriagada et al. (2002) and Mpodozis et al. (2005) present evidence that during the late Cretaceous, the Salar Basin began in a compressional setting as a foreland basin linked to the initial stages of uplift of the Cordillera de Domeyko. They emphasize that the basin-forming event was the inversion of the Jurassic–early Cretaceous extensional Tarapacá backarc Basin, which dominated the Mesozoic paleogeography of northern Chile. Several authors suggest that a major stage of evolution of the Salar de Atacama Basin occurred in an Oligocene tectonic environment

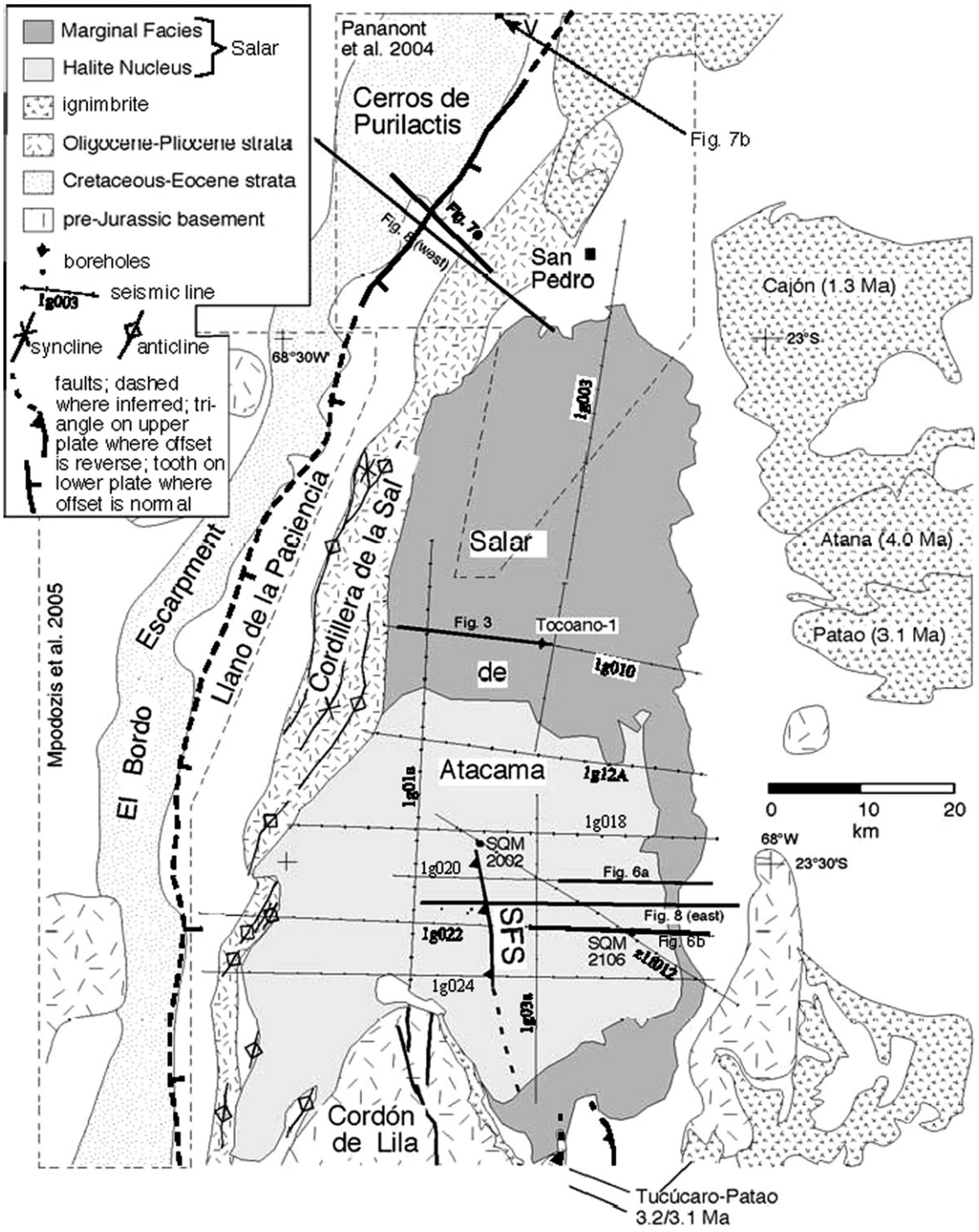

Fig. 2. Map of Salar de Atacama Basin showing principal physiographic features, key geologic units, locations of seismic lines, boreholes, and areas of companion studies (within polygons limited by dashed lines) of a northern suite of seismic lines and outcrops (Pananont et al., 2004) and of western outcrops and geochronology (Mpodozis et al., 2005). Within the Salar, halite-generating and marginal (mixed clastic and gypsum-flat) depositional environments are differentiated. The white areas west of the Salar are mostly surfaced by unconsolidated deposits, whereas the white areas east of the Salar are dominated by volcanic rocks other than ignimbrites. Ages (Ma = millions of years) are indicated for major ignimbrite sheets that help constrain the ages of seismic sequences in the Salar subsurface. Laterally persistent folds in the southern and central Cordillera de la Sal are shown, but in the northern Cordillera de la Sal, a complex set of domes and basins with short hinges of diverse orientation are not mapped. Faults mapped within (SFS = Salar fault system) and south of the Salar offset Pliocene and younger units.

characterized by strike-slip deformation (Macellari et al., 1991; Wilkes and Görler, 1994).

We evaluate the Cenozoic Salar de Atacama Basin, focusing especially on the Oligocene to modern basin evolution. Although our focus is on the little deformed region underlying the modern Salar, we also incorporate key information from the outcrops along its northwestern and western margin. We base this analysis on the extensive set of

seismic data acquired by ENAP (Chile's national oil company) and industrial partners, three key boreholes in Salar de Atacama (Muñoz and Townsend, 1997; Jordan et al., 2002a,b), and a comprehensive database of ash (ignimbrite) chronology available for the outcrop stratigraphy (Ramírez and Gardeweg, 1982; Mpodozis et al., 2000; Blanco et al., 2000; Lindsay et al., 2001; Mpodozis et al., 2005).

The Salar de Atacama Basin occupies approximately 8000 km^2 in the western two-thirds of a closed-drainage basin in which the modern 3000 km^2 Atacama Salar (salt pan) rests (Fig. 1). First, we evaluate the length of time over which there existed similar spatial limits to the basin. Second, we differentiate times with active tectonic subsidence from times in which strata passively filled a preexisting topographic low, which we deduce on the basis of (1) the locations of faults relative to depocenters and their displacement magnitudes, (2) onlap and truncation patterns of reflections as indicators of tilting, and (3) patterns of sediment thicknesses. Third, we identify the tectonic controls on subsidence.

2. Database and methods

During the 1980s, ENAP and its partner companies collected seismic reflection profiles over much of the Salar de Atacama Basin for the purpose of oil exploration. Data within the Salar consist of a series of east–west-oriented lines (spaced 5 km apart in the south-central region and slightly farther apart in the northern sector) and tie-lines of N–S, NW–SE, and NE–SW orientations (spaced at variable intervals, typically 10–15 km). We report the Cenozoic stratigraphy imaged by this grid of seismic data (Fig. 2). Pananont (2003) and Pananont et al. (2004) report on a second grid of seismic lines that crosses the northwestern sector of the basin, inclusive of the Cordillera de la Sal and the eastern border of the Cordillera de Domeyko; this paper draws from their results.

The 5.5 km deep Toconao-1 borehole, drilled in a position adjacent to one of the seismic lines near the center of the Salar (Fig. 2), traverses the Cenozoic strata (Fig. 3C) and provides constraints on lithologies and the conversion between the depth and seismic two-way travel time (Fig. 4) (Muñoz and Townsend, 1997). Unfortunately, the well cuttings provide few constraints on the ages of the nonmarine clastics. Subsurface age data are also provided by a set of cores drilled for a brine-mining prospect, owned by SQM Corporation. This core set yields excellent coverage for the upper 30–40 m of the basin fill in much of south-central Salar, with several cores reaching hundreds of meters depth (Bevacqua, 1991). Core 2002, 500 m in length, achieves the deepest penetration (Fig. 2). Core 2106, 390 m, penetrates an ignimbrite along the eastern margin of the Salar, for which Bevacqua (1991) reports a K–Ar age, a key chronological constraint throughout the seismic grid. Bobst et al. (2001) and Lowenstein et al. (2003) provide detailed studies of three cores and chronological data for the most recent 325,000 years. Jordan et al. (2002a,b) correlate major ignimbrites exposed along the north, east, and southeastern borders of the Salar de Atacama (Ramírez, 1979; Ramírez and Gardeweg, 1982; Lindsay et al., 2001) with uncommonly high amplitude and low frequency seismic reflections, which led to approximate age assignments of the Pliocene seismic stratigraphic units.

We base our subsurface mapping approach on the definition of unconformity-bounded stratigraphic sequences. We map unconformities on each of the seismic lines, recognized on the basis of truncations and lap-out relations of reflections. We treat the surfaces represented by the unconformities and their conformable lateral equivalents, traced among the multiple seismic lines, as stratigraphic sequence boundaries (i.e., Cross and Lessenger, 1988). The two-way travel time duration of each stratigraphic sequence (the unit contained between two successive sequence boundaries) may be transformed to depth on the basis of velocities in the Toconao-1 borehole. Thicknesses were mapped and manually contoured. Our results indicate that correlations between outcrop and subsurface stratigraphy (Fig. 4) are constrained by either (1) borehole and ignimbrite data (most useful for shallow units) or (2) comparison of the character of change at the subsurface unconformities with the unconformities exposed west and north of the Salar.

3. Salar subsurface: stratigraphic units and spatial patterns

Six major stratigraphic sequences are identified in the seismic data and traced throughout the Salar region (Figs. 3 and 4). We use letters to denote the sequences (F, G, H, J, K, and M) and describe their seismic characteristics, properties in the borehole, and spatial extent from the youngest (M) to the oldest (G) of the five sequences characterized by coherent reflections that indicate sedimentary rocks. "F" is used for the seismic "basement" of poorly reflective rocks, on which we do not elaborate. Because the sequence boundaries we use are not identical to the boundaries between sequences A–F described by Muñoz and Townsend (1997) and Muñoz et al. (2002), we intentionally choose an independent lettering system. The G–M sequence designations have been used by Pananont et al. (2004) and Arriagada (2003). With the exception of the youngest unit, whose age is known by direct means, we discuss correlations of these subsurface sequences to units that crop out west of the Salar in a subsequent section. Although opposite to the order used in most stratigraphic studies, we describe the units from upper to lower to respect the order of diminishing reliability of seismic stratigraphy, a result of the progressive decrease in resolution of the data from top to bottom.

3.1. Subsurface sequence M (halite unit)

This unit encompasses all the sedimentary rocks from the Salar surface to a base where a major lithologic change exists in the Toconao-1 borehole (Fig. 3A). Halite dominates above a depth of 980 m in Toconao-1, though the

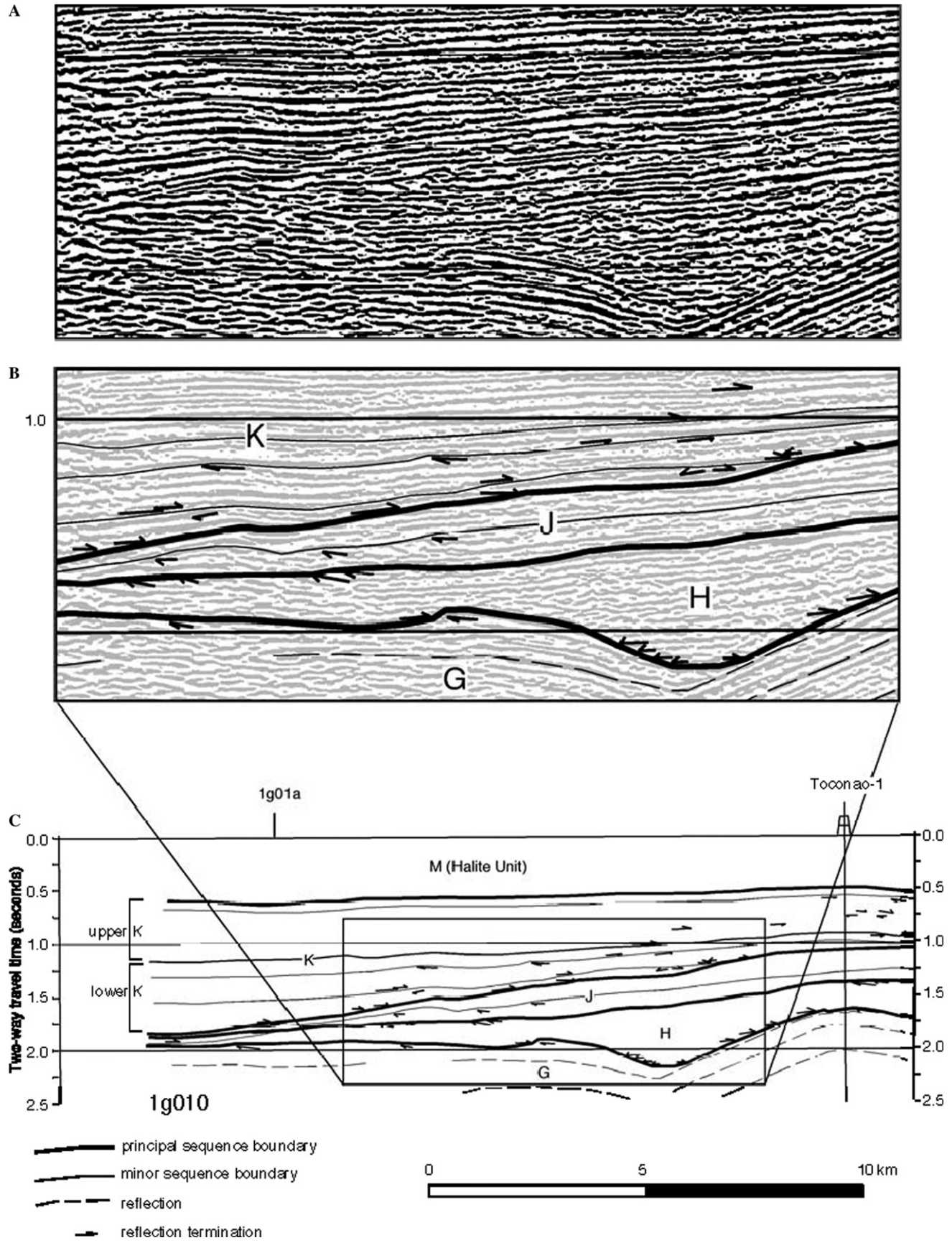
A
B
1.0
K
J
H
G
1g01a
Toconao-1
C
0.0
0.5
1.0
1.5
2.0
2.5
Two-way travel time (seconds)
M (Halite Unit)
upper K
lower K
K
J
H
G
1g010
principal sequence boundary
minor sequence boundary
reflection
reflection termination
0
5
10 km

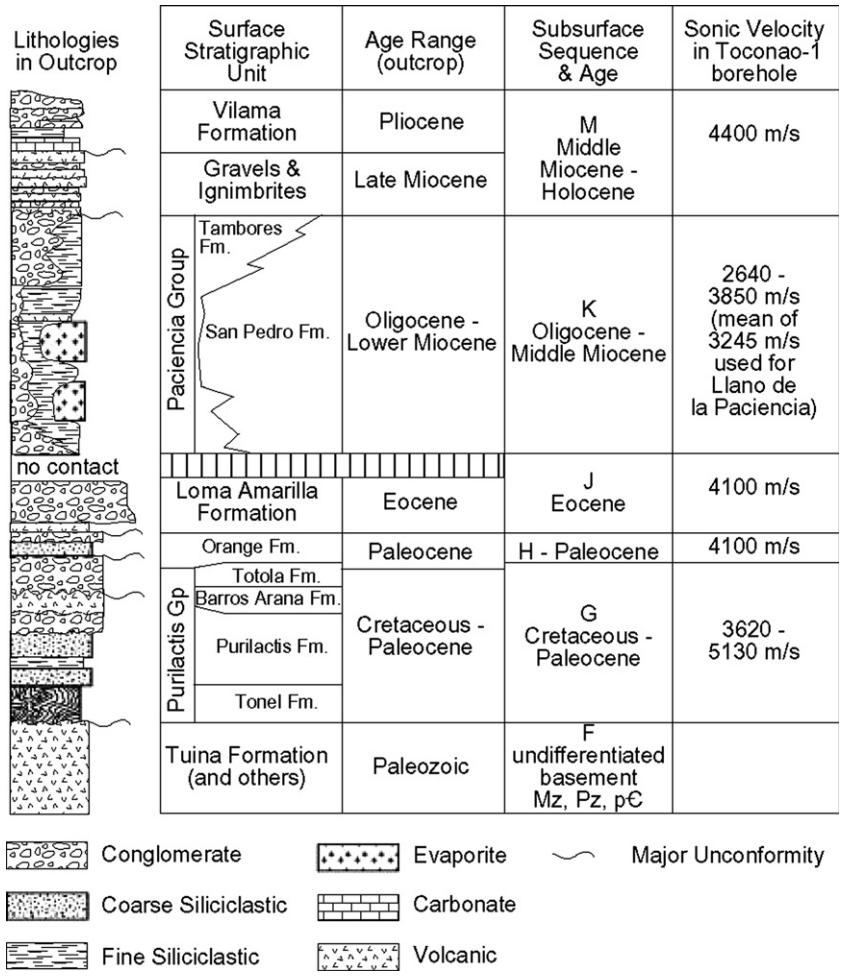

Fig. 4. Correlation of surface and subsurface stratigraphy of the Salar de Atacama Basin and seismic velocity of each unit at the Toconao-1 borehole (see Fig. 2) (after Pananont et al., 2004; Ramírez and Gardeweg, 1982; Wilkes and Görler, 1994; Mpodozis et al., 2000, 2005; Muñoz et al., 2002).

interval from 480 to 620 m contains fine-grained clastic detritus interbedded with halite. Abundant borehole data in the southern Salar region demonstrate that halite is the dominant lithology south of the Toconao-1 well. Pananont et al. (2004) determine from seismic velocities of refractions from a shallow layer (measured from first-breaks on common midpoint gathers) that halite is also present in the shallow subsurface near the north end of the Salar. Our unit M is identical to Muñoz and Townsend's (1997) unit F, which they assign to the Quaternary; that correlation later was revised (Jordan et al., 2002a,b), as we describe in the next section.

We trace the base-of-halite horizon along seismic reflections throughout the Salar; it varies from less than 400 m depth in the southwest extreme to greater than 1800 m in the northern extreme (Fig. 5A). In the northern part of the Salar, this sequence thickens toward the north-northeast trending Cordillera de la Sal. In the southern half of the Salar, the thickness pattern is controlled by the north-northwest-trending Salar fault system. Near the middle of the Salar, the Salar fault system consists of a single major blind reverse fault across which sequence M thickens abruptly from 625 to 750 m on the west side to 900–1500 m on the east (Fig. 5A). That single fault splays southward to a set of blind reverse faults with moderate offset. These blind reverse faults control sequence M thickness and are a northward continuation of the emergent Plio–Pleistocene reverse faults that cut the Cordón de Lila and the Tilocalar valley (Gardeweg and Ramirez, 1982; Kuhn et al., 1997). A similar set of buried reverse faults, the Peine faults, affects

Fig. 3. (A) Seismic lines and (B–C) line drawings of seismic lines representative of the central Salar de Atacama Basin, presented in the time domain. Locations shown in Figs. 2 and 5a. The boundaries of the five major stratigraphic units are shown, plus second-order subsequence boundaries. (A) Seismic data and (B) interpretation of small sector of line 1g010 (see c for location), illustrating the terminations of seismic reflections that lead to the stratigraphic subdivisions of sequences and subsequences. (C) Interpretation of the western part of the Salar as imaged on 1g010 and the relationship of the Toconao-1 borehole to the seismic interpretation. Major changes through time in subsidence style are expressed by the progression from unit H (localized depocenters controlled by underlying fold geometry) to unit J (broadly distributed but rotated to the east during the time of the unconformity that underlies K) to unit K (thickens to west) to unit M (similar thicknesses).

sequence M along the eastern margin of the Salar (Fig. 6A), though their typical offset (up-to-the-west) is antithetic to the long-wavelength westward thickening of sequence M, and their impact on thickness patterns is minor. Along the eastern margin of the Salar, the base of sequence M is inclined approximately 2–4° to the west (segments a–c, Fig. 5A) along profiles that reflect regional dip rather than short-wavelength deformation related to the Peine faults.

The halite unit consists of at least eight subsequences, seismically defined by discordant relations among reflections. A majority of the unconformable relations occur in the vicinity of the Salar fault system, typified by truncations of horizons rotated during folding and onlap across short-lived fault scarps (Jordan et al., 2002a,b). Comparison of thicknesses and onlap relations of the individual subsequences reveals that displacement on the Salar fault system occurred episodically over an interval that spans the last 5–10 Ma (Jordan et al., 2002a,b). We posit that most of the unconformities resulted from tectonic activity, though volcanic eruptions and climate change likely contributed to the development of certain unconformities.

3.2. Subsurface sequence K

The second major sequence, K, is defined at its top by a change from halite to detrital clastic sediments in the Toconao-1 borehole. The base of sequence K is a prominent unconformity in the western part of the Salar, marked by onlap of a west-dipping surface (Fig. 3A). This surface truncates reflectors in unit J that appear to define broad, gentle folds. Below the northeastern Salar, the erosional unconformity under unit K is slightly angular, as it is above the gentle folds in unit J.

Sequence K includes several subsequences separated by gentle angular unconformities. At the scale of the entire basin, the most prominent is a regional horizon of westward tilting, which divides upper and lower subsequences (Figs. 3 and 6). This unconformity is especially well developed near the northern and eastern borders of the Salar, where lower sequence K is erosionally truncated (Fig. 6A); in the western Salar, only gentle onlap is evident (Fig. 3). Furthermore, the lower subsequence contains at least three higher-order subsequences (Fig. 3), each of which is thin and widespread, indicating that the basin topography changed little between the times of deposition of successive subsequences. The base of these higher-order subsequences onlapped only as far east as what is now the center of the Salar. Consequently, borehole Toconao-1 does not include rocks within the lowest unconformity-bounded subsequence in unit K.

Our sequence K includes much of Muñoz and Townsend's (1997) sequences E–C, corresponding to a depth of 980 m to approximately 2100 m (1060 ms TWTT) in the Toconao-1 borehole. Upper sequence K corresponds to Muñoz and Townsend's (1997) sequence E and much of sequence D, in a depth range between 980 m and approximately 1800–1860 m in the deep borehole (Fig. 3C). Lower sequence K comprises the lower 200 m of Muñoz and Townsend's (1997) sequence D and upper 100 m of their sequence C. For upper sequence K at the borehole, the upper 600 m is dominated by claystone with minor sandstone and anhydrite, and the lower 250 m is dominated by conglomerates of volcanic clasts. Lithologies between 1860 and 2100 m, in lower sequence K, include a reddish volcanic conglomerate as well as minor sandstone and claystone.

3.3. Subsurface sequence J

Stratigraphic sequence J is widespread in the Salar subsurface. This sequence corresponds to the depth range between approximately 2100 m and 2300 m in the Toconao-1 borehole (Fig. 3C), for which the lithology is a multicolored sandstone with common interbeds of conglomerate and claystone. Our sequence J corresponds to the lower two-thirds of Muñoz and Townsend's (1997) sequence C.

The unconformable boundary between units K and J is well defined in the west-central and southwestern sectors of the Salar (Fig. 3). Over a distance of at least 15 km, unit J was truncated to progressively deeper stratigraphic horizons to the west at an angle of approximately 3° with respect to bedding, suggesting eastward tilt prior to the time of unit K.

Stratigraphic sequence J overlies sequence H above a prominent erosional surface. Locally, that erosional unconformity cuts deeply into underlying sequence H, as shown near the western border of the Salar in Fig. 3. Sequence J reflections parallel the underlying unconformity, but reflections in sequence H dip variably to the east and west below the basal unconformity, defining broad folds.

Sequence J currently thins gradually to the west and east from a pair of maxima in the central and northern Salar (Fig. 5C). For the central maximum, this thickness pattern is clearly a consequence of erosion (which removed the top of sequence J in the west), as well as depositional topography (pinching out eastward by onlap at its base).

Fig. 5. Thickness maps of the four major stratigraphic intervals of Cenozoic units, contoured in meters. (A) Simplified from Jordan et al. (2002a) for sectors in the Salar, based on automated contouring of all ENAP's seismic lines (denser grid than shown). (B–D) Based on seismic lines whose positions are shown and reports from the literature of thicknesses in outcrop of correlative units. The subsurface data for areas northwest of the Salar are from Pananont et al. (2004), and thicknesses of units in outcrop (Mpodozis et al., 2005) permit generalized contours in the far western part of the basin. Not all faults are shown. (A) Unit M, 10–0 Ma. (B) Unit K, 30–10 Ma. (C) Unit J, 42–30 Ma. (D) Unit H, Paleocene. Folds in underlying well-stratified Cretaceous units (shown in D), where constrained by intersections of two seismic lines, typically trend NW. In A, line segments a, b, and c (along seismic lines 1g002, 1g006, and 1g018) illustrate profiles where the base of M dips 2.0°, 3.9°, and 2.5° west, respectively.

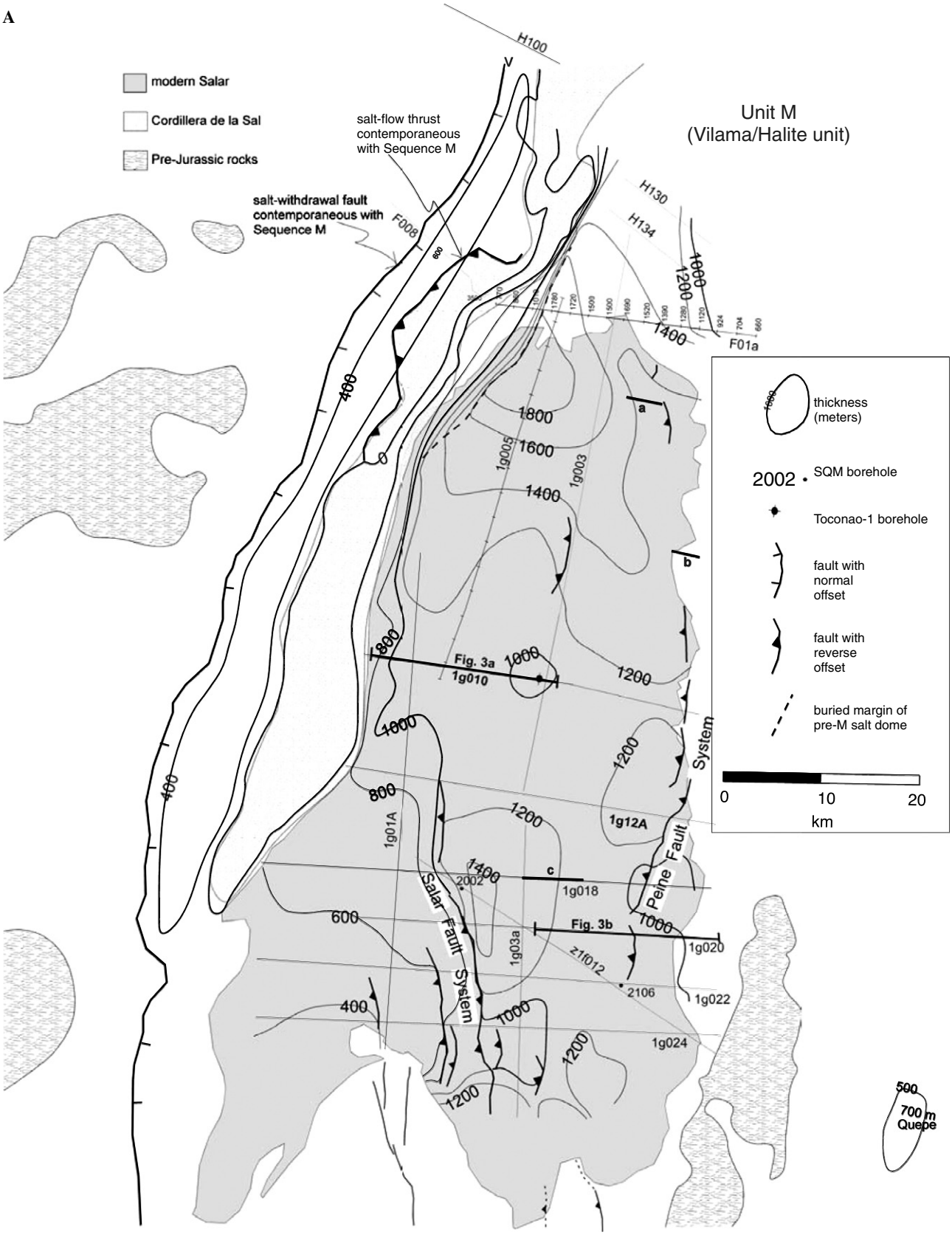
A
modern Salar
Cordillera de la Sal
Pre-Jurassic rocks
salt-flow thrust contemporaneous with Sequence M
salt-withdrawal fault contemporaneous with Sequence M
F008
Unit M
(Vilama/Halite unit)
H100
H130
H134
F01a
thickness (meters)
2002 SQM borehole
Toconao-1 borehole
fault with normal offset
fault with reverse offset
buried margin of pre-M salt dome
0 10 20
km
Fig. 3a
Fig. 3b
1g010
1g005
1g003
1g01A
1g12A
1g018
1g03a
1g020
1g022
1g024
z1f012
2002
2106
Salar Fault System
Peine Fault System
Quepe
500
700 m

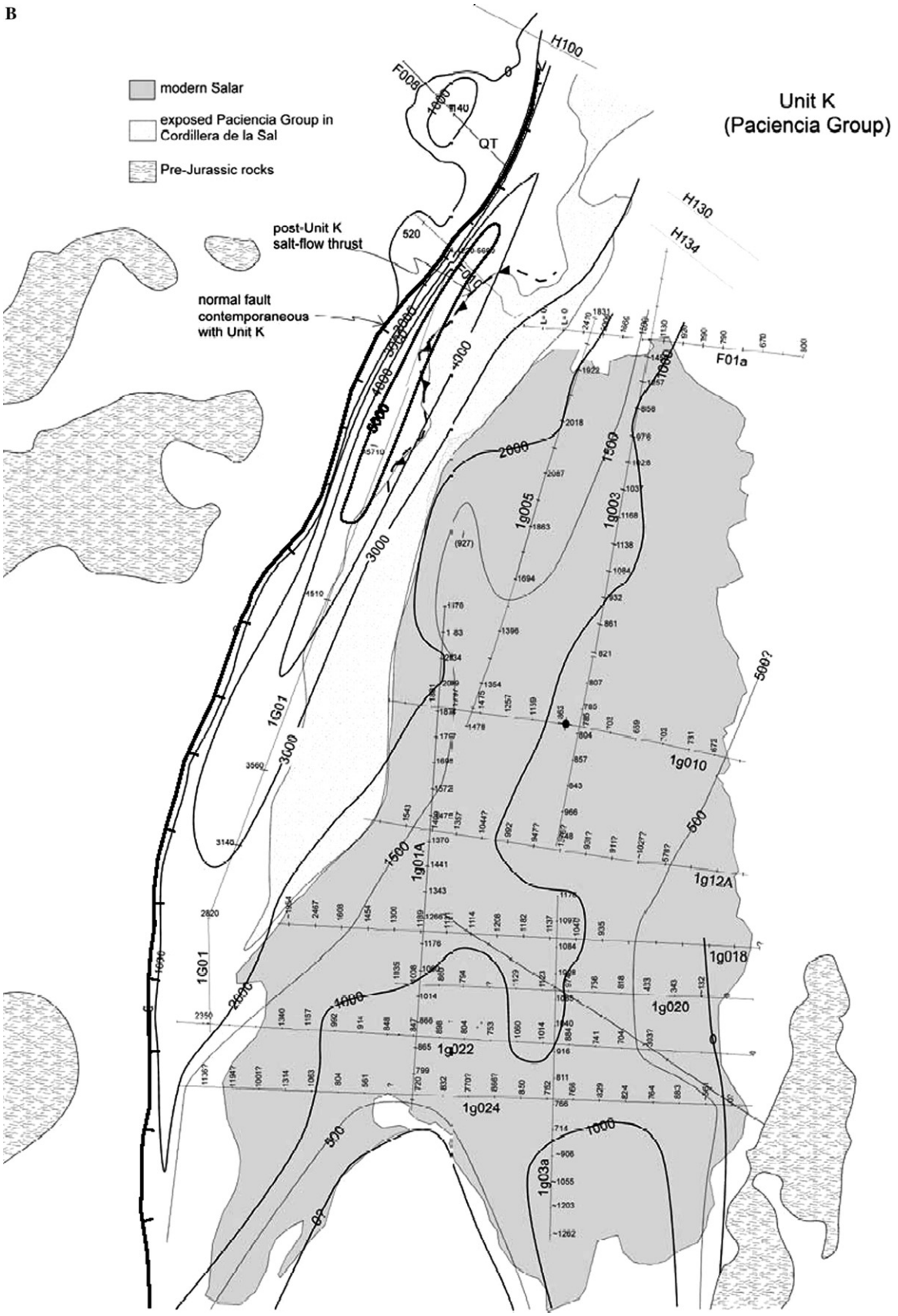

Fig. 5 (*continued*)

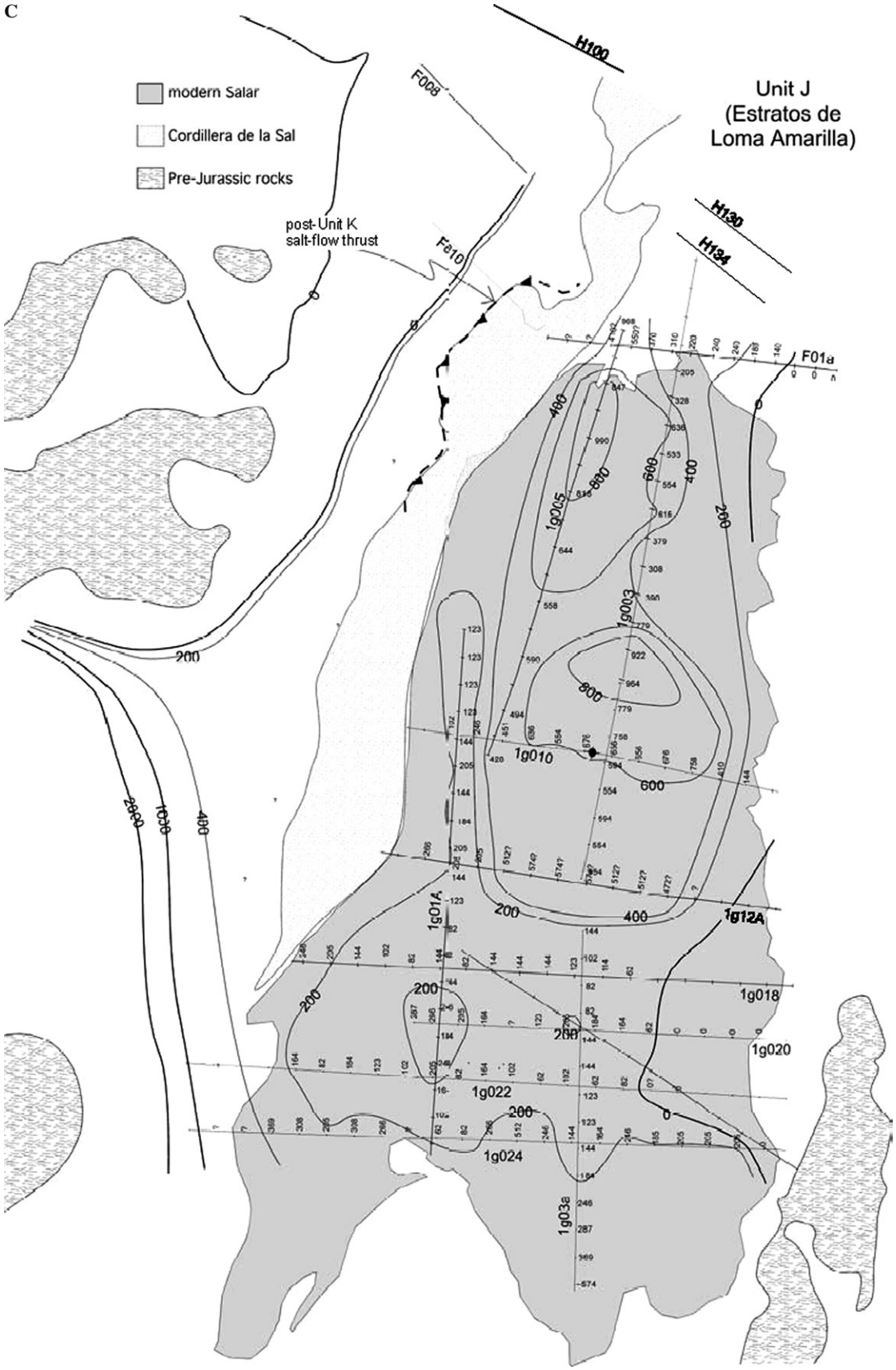

Fig. 5 (*continued*)

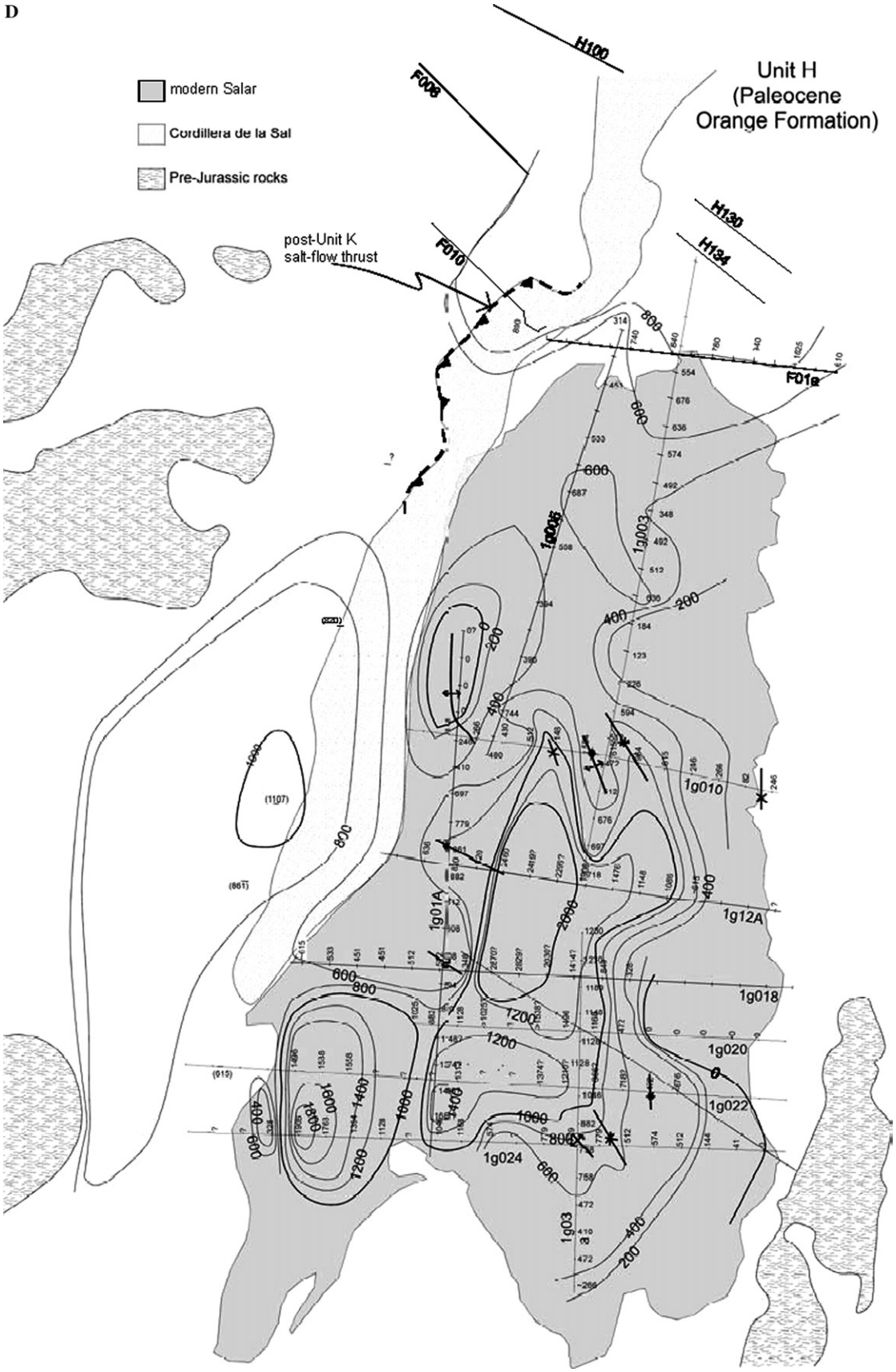

Fig. 5 (*continued*)

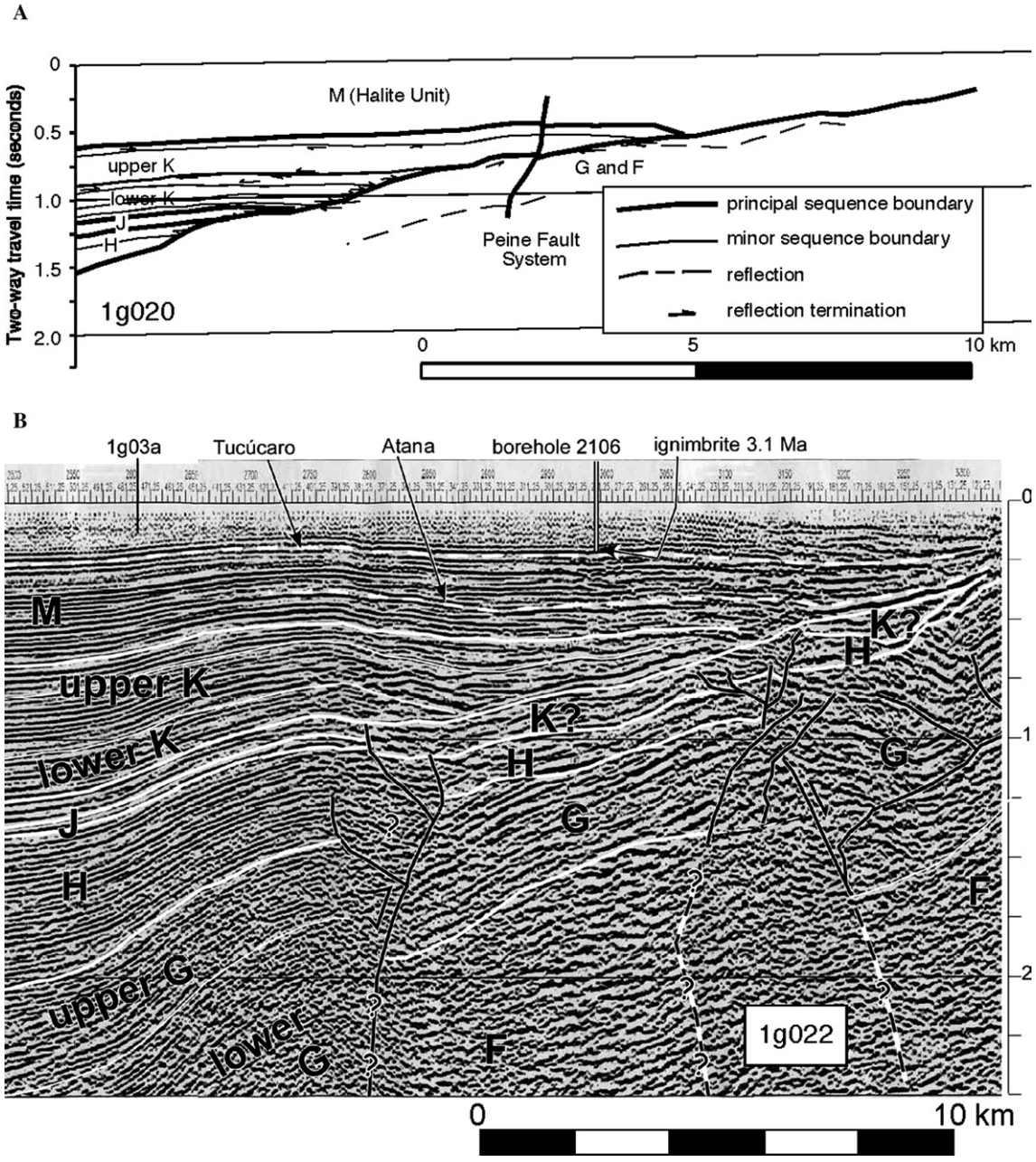

Fig. 6. Line drawing and seismic data representative of the eastern margin of the Salar de Atacama Basin, presented in the time domain. Locations shown in Figs. 2 and 5a. The boundaries of the five major stratigraphic units (M–G) and of basement (F) are shown, plus second-order subsequence boundaries. (A) Seismic line 1g020 (line drawing) typifies the eastern margin and illustrates the onlap of Cenozoic units (H–M) over the deformed Mesozoic Purilactis Group strata (G). There was steady but modest change in the position of the basin margin between the times of units H through lower K but significant migration of the margin to the east during times of upper unit K and M. Also evident is the very small degree of Cenozoic deformation along the Peine fault set. (B) Seismic line 1g022 illustrates the area adjacent to the Peine basement ridge, the only pre-late Miocene rocks exposed along the eastern margin of the Salar Basin, as well as the relationship of the dated ignimbrite drilled in borehole 2106 with the seismic profile. Dashed lines show the positions of two other extensive ignimbrites, the Tucúcaro and Atana, as interpreted by Jordan et al. (2002a,b). Two groups of faults of the Peine fault set that cut units F through K began as normal faults bounding Cretaceous subbasins. Both eastern and western groups of faults were active during unit H and K deposition, with a mixture of local reverse and normal offsets. Only the western group of faults experienced small degrees of reverse displacement, causing folding at shallow depth, during deposition of the upper 100 ms of unit K and throughout deposition of unit M.

3.4. Subsurface sequence H

This unit fills the relief above an erosional surface whose shape mimics folded strata below the unconformity (Fig. 3). The basal unconformity is marked by erosional truncation of the underlying, folded strata and onlap across steeply inclined erosional surfaces (Muñoz et al., 1997). The top of the unit is an erosional unconformity that cuts broadly across gently tilted reflectors. In the Toconao-1 borehole, this unit is represented from 2300 to 2800 m

depth by volcanoclastic sandstone, with subsidiary conglomerate and claystone (Muñoz and Townsend, 1997). This unit corresponds to sequence B of Muñoz and Townsend (1997).

The similarity in form between the erosional contact at the base of this unit and the shape of the underlying folded strata (Fig. 3) implies that little erosion of the large amplitude folds occurred before long-term accumulation of sequence H filled the structural relief. Subsurface sequence H ranges in thickness from roughly 2000 m in the troughs of the largest synclines to zero over some anticlinal crests (Fig. 5D). This unit pinches out in the eastern part of the Salar against structural highs formed by the deformation of sequence G (Fig. 6).

3.5. Subsurface sequence G

Strata below unit H are well defined and clearly folded below some parts of the Salar (e.g., Figs. 3 and 6); however, beneath much of the Salar, it remains ambiguous whether the sub-H units are layered, due to insufficient seismic resolution. Adequate seismic quality below unit H enables us to identify well-stratified units as sequence G; we label clearly unstratified units as sequence F. Muñoz and Townsend (1997) identify our unit G as sequences A1 and A2. Sequence G is thousands of meters thick below much of the central and western Salar but thins to a few hundred meters or zero thicknesses in the northeastern Salar, along parts of the Salar fault system, and locally in the southeastern Salar region. To date, the details of the spatial distribution and thickness patterns of sequence G are not fully mapped.

In the Toconao-1 borehole, the range 2800–3720 m consists of red claystone and sandstone. Below 3720 m exists a 100 m thick interval with thin limestone beds intercalated with claystone and siltstones that include rare glauconite grains, which may indicate a shallow, quiet marine depositional environment (ENAP, 1990, unpublished report). Mpodozis et al. (2005) postulate that these limestones accumulated during a regional Maastrichtian transgression.

4. Correlation of subsurface stratigraphy of the Salar with exposures west of the Salar

Recent and ongoing studies of units exposed west and north of the Salar de Atacama and chronologic studies of the upper units below the Salar suggest significant revisions to the published correlations of the subsurface sequences presented by Muñoz and Townsend (1997). The principal controls on the proper correlations of these subsurface units relate to units that crop out in the eastern Cordillera Domeyko, Llano de la Paciencia, and Cordillera de la Sal in several ways.

First, recognition of ignimbrites in subsurface sequence M requires that it be younger than the oldest major late Cenozoic ignimbrite, which leads to the interpretation that its base may be dated between 5 and 10 Ma (Jordan et al., 2002a,b). The top of unit M is of late Holocene age (Bobst et al., 2001). We summarize the details of the ignimbrite correlations next (Jordan et al., 2002a,b).

Several strong, low frequency, negative polarity reflections interfinger with sequence M along the eastern flank of the Salar (Fig. 6B). Six meters of the Patao Ignimbrite were traversed and the ignimbrite's age confirmed in SQM borehole 2106 (Bevacqua, 1991). Studies in neighboring exposures to the east (Fig. 2) reveal that two ignimbrites, the 3.1 ± 0.2 Ma Patao and 3.2 ± 0.7 Ma Tucúcaro, were produced by two different eruptions (Ramírez and Gardeweg, 1982) and likely overlie each other in the subsurface. On seismic lines 1g022 and Z1f012 occurs a prominent seismic reflection (trough) of low frequency and excellent lateral continuity, immediately below the two-way travel time appropriate to the cored ignimbrite; we correlate the prominent reflection to the Tucúcaro Ignimbrite (Fig. 6B). Below the Tucúcaro (?)Ignimbrite occur several other prominent reflections, the most prominent and widespread of which we interpret as the 4.0 Ma Atana Ignimbrite (Gardeweg and Ramírez, 1987; Lindsay et al., 2001). Other reflections typical of ignimbrites occur at greater depth along the eastern margin of the Salar. Because ignimbrites that range in age between 5.8 and 10 Ma are known in isolated outcrops east of the Salar (Ramírez and Gardeweg, 1982; Lindsay et al., 2001) and are abundant north of the Salar (Ramírez and Gardeweg, 1982; Mpodozis et al., 2000), the base of the halite unit is bracketed as older than 4.0 Ma and perhaps as old as 10 Ma. In this text, we simplify this information by reference to its basal age as 5–10 Ma while maintaining that an uncertainty of a few million years exists on the basal age of unit M.

Second, ages of the oldest subsurface sequences are constrained by geometric similarities of unconformities with the Cretaceous and Paleogene series exposed west of the Salar. Arriagada (1999) and Mpodozis et al. (2005) greatly increase the resolution of ages of the Cretaceous Purilactis Group (Tonel, Purilactis, Barros Arana, and Totola formations, in ascending order), Paleogene Orange Formation, and Loma Amarilla Formation along El Bordo escarpment (Figs. 2 and 4). Sequence H onlaps prominent relief above major folds. Along El Bordo escarpment, a similar discordant relationship separates overlying nonmarine conglomerates and sandstones of the Orange Formation from the underlying Upper Cretaceous Purilactis Group (Arriagada, 1999; Mpodozis et al., 2005). Therefore, we make a physical correlation of the Orange Formation–Purilactis Group unconformity with the boundary of sequences H and G. Interbedded andesitic lava flows in the Orange Formation are dated (K/Ar whole-rock) as 57.9 ± 1.9 and 58.0 ± 3 Ma (Gardeweg et al., 1994), whereas Totola Formation lavas below the unconformity yield K/Ar ages of 66–68 Ma (Mpodozis et al., 2005). Thus, the exposed Orange Formation is well constrained within the Paleocene. Independently, the identification of scarce Coniacian–Maastrichtian microfauna in the upper 900 m of

unit G in the Toconao-1 borehole (ENAP, 1990, unpublished report) lends support to the interpretation that sequence H, unconformable above folded sequence G, has the same stratigraphic position as the Paleocene Orange Formation.

Third, in outcrop west of the Southern Salar, the Paleocene Orange Formation is capped by a prominent erosional unconformity, above which widespread and very coarse conglomerates of the Loma Amarilla Formation occur. An ash-rich pyroclastic layer at the base of the Loma Amarilla has been dated (biotite, $^{39}Ar/^{40}Ar$ plateau ages) at 43.8 ± 0.5 and 42.2 ± 0.9 Ma (Hammerschmidt et al., 1992). Where the Eocene Loma Amarilla conglomerates overlie the Paleocene Orange Formation, the Paleocene strata dip more steeply than the overlying unit. Likewise, sequence J overlies unit H in the subsurface above a prominent erosional surface that cuts deepest into sequence H in the western part of the Salar. This scenario leads us to correlate sequence J with the Eocene Loma Amarilla Formation.

Fourth, strongly folded Oligocene to lower Miocene Paciencia Group strata are overlain unconformably by 17 Ma lavas locally and, more broadly, a stack of upper Miocene ignimbrites to the north and northwest of the Salar, in the northern Llano de la Paciencia and Cordillera de la Sal (Fig. 2) (Ramírez and Gardeweg, 1982; Marinovic and Lahsen, 1984; Mpodozis et al., 2000). The 10 Ma Artola Ignimbrite is the base of the ignimbrite and siliciclastic section, a few tens to hundreds of meters thick, that overlies the Paciencia Group (Ramírez, 1979; Marinovic and Lahsen, 1984; Flint et al., 1993; Mpodozis et al., 2000). Locally, in the single location with the 17 Ma lavas, the duration of the angular unconformity is about 3 Ma, but in most of the Cordillera de la Sal and Llano de la Paciencia, approximately 10–12 m.y. of time, including the entire middle Miocene interval, is omitted at that unconformity. In the subsurface of the northern Salar, the lower major subsequence of K is broadly folded, truncated above by an erosional unconformity, and overlain by the upper major subsequence of K, which in turn is only folded at the margins of the Cordillera de la Sal. Thus, there is a similarity between the structural relations across the intra-K unconformity beneath the Salar and the unconformity above the Paciencia Group in outcrop. Nevertheless, no similarity appears to exist between the temporal magnitude of the exposed early and middle Miocene unconformity and either the intra-K unconformity or the sequence boundary at the top of K, because the top of sequence K is conformable with the approximately 5–10 Ma base of sequence M beneath much of the Salar (Figs. 3 and 6). Therefore, sequence K is bracketed as younger than Eocene sequence J and older than the 5–10 Ma base of unit M and probably includes both the Paciencia Group and the time interval of the exposed post-Paciencia unconformity, that is, approximately 30–10 Ma.

Unfortunately, the cuttings and sidewall cores from the Toconao-1 borehole yield very sparse biostratigraphic results above 2810 m (ENAP, 1990, unpublished report). The resolution of palynological correlations is far less than the temporal resolution needed to differentiate among the four Cenozoic-age units. Muñoz et al. (2002) report apatite fission-track ages for detrital clasts derived from various depths in the Toconao-1 borehole, which suggest partial to total annealing at depths greater than 2500 m. However, at shallower horizons, the apatite fission-track ages may represent the cooling ages of the detritus prior to delivery to the Salar de Atacama Basin and thus place maximum ages on deposition of the unit carrying the detritus. Apatite fission-track ages of four horizons suggest depositional ages younger than 56 Ma within sequence J (cf. 43.8 ± 0.5 and 42.2 ± 0.9 Ma for interbedded ashes in outcrop near the base of the Loma Amarilla Formation) and younger than 46 Ma in sequence K (cf. 28–20 Ma ash interbeds within the outcropping Paciencia Group). These constraints are consistent with the outcrop correlations suggested previously.

In summary, the uppermost major sequence (M, halite unit) is approximately equivalent in age to the series of ignimbrites and siliciclastic units exposed north of the Salar (i.e., Artola, Sifón, Yerba Buena, and Pelón ignimbrites), the Vilama Formation, and the overlying unconsolidated deposits of the northern Cordillera de la Sal and Llano de la Paciencia area of approximately 10–0 Ma (Blanco et al., 2000). Despite their age equivalence, the siliciclastic alluvial plain, fluvial, and lacustrine Vilama Formation contrasts markedly in lithology with the evaporite-dominated subsurface sequence M. We correlate the second unit, sequence K, with the unconformity that separates the ignimbrite and gravel units from the Paciencia Group, as well as with the siliciclastic and evaporitic Oligocene–lower Miocene Paciencia Group. We correlate unit J with conglomerates of the Eocene Loma Amarilla Formation. The lowest unit that we mapped comprehensively, unit H, onlapped a surface of high relief above prominently folded Upper Cretaceous units, the same relation mapped in outcrop at the base of the Paleocene Orange Formation described by Arriagada (1999) and Mpodozis et al. (1999, 2005).

5. Stratigraphic summary of Salar de Atacama Basin and comparison to structural evolution of Cordillera Domeyko–Cordillera de la Sal

These new correlations lead to a much more complete description of basin evolution because they enable us to combine subsurface relations with constraints from the surface geology and absolute dates on various interbedded volcanics. Other available constraints on the basin's evolution, established by surface and subsurface studies of the region west and northwest of the Salar (e.g., Macellari et al., 1991; Hooper and Flint, 1987; Mpodozis et al., 2000; Wilkes and Görler, 1994; Pananont, 2003; Pananont et al., 2004) and surface studies along El Bordo escarpment southwest of the Salar (Arriagada et al., 2002; Mpodozis

et al., 2005), in combination with this new study of the Salar subsurface stratigraphy, suggest a regional Cenozoic structural history that explains both exposed and subsurface patterns. We compile observations within the basin pertinent to distinguishing the causes of accommodation space in Table 1.

Pananont et al. (2004) correlate the subsurface relations imaged in seismic data with the overlying surface geology across the Cerros de Purilactis, Llano de la Paciencia, Cordillera de la Sal, and northernmost part of the Salar de Atacama. Their principal findings include several points.

First, a boundary exists just east of the foot of the Cerros de Purilactis across which the Paciencia Group thins abruptly to the west. The boundary is a north-northeast-trending surface that dips steeply to the east (Fig. 7A). We interpret this feature as a normal fault (Paciencia Fault) tectonically generated during the Oligocene.

Second, near the northern margin of Salar de Atacama, the structural relief on the top of the Paciencia Group between Llano de la Paciencia and Cordillera de la Sal is 1 km down-to-the-west, and between Cordillera de la Sal and the immediately adjacent Salar, it is 1 km down-to-the-east. These vertical offsets must be contemporary with and/or younger than the post-Paciencia Group unconformity and 10–5 Ma ignimbrite series. These offsets result from slight tectonic thrusting east of Cordillera de la Sal (Tulor Fault) combined with significant salt withdrawal from the Llano de la Paciencia associated with diapiric uplift in the Cordillera de la Sal.

5.1. Sequence M/Vilama Formation/ignimbrites

The late Miocene–Pliocene evolution of the Salar de Atacama Basin (Fig. 8F) includes deformation along the Cordillera de la Sal and Llano de la Paciencia, well defined in Vilama Formation history (Blanco et al., 2000); the generation of buried reverse faults in the southern and eastern Salar (Jordan et al., 2002a,b); and large ignimbritic eruptions from collapse calderas east and northeast of the Salar (i.e., La Pacana Caldera; Gardeweg and Ramírez, 1987; De Silva, 1989b; Lindsay et al., 2001). Curiously and conflicting with standard assumptions about deposition in volcanically or tectonically active domains, this deformation and volcanism resulted in a sediment supply dominated by dissolved load rather than detritus.

In the Cordillera de la Sal just beyond the NW corner of the Salar, the Vilama Formation at Cerro Mármol exhibits growth unconformities related to folding (Blanco et al., 2000). Strata in the Vilama Formation are also strongly folded along the eastern border of Cordillera de la Sal. This field evidence of Pliocene deformation and uplift is consistent with the westward thickening of sequence M beneath the Salar toward the eastern margin of the northern Cordillera de la Sal (Fig. 5A). In the northern Cordillera de la Sal, salt flow dominates the Pliocene deformation. This migration of a major body of salt on an inclined trajectory to the west (Fig. 8F) created a major overhang of Paciencia Group salt (the modern area of domes and swales in Cordillera de la Sal) above units H–K (Fig. 5B–D) (Pananont et al., 2004). The major tectonic fault activity occurred along a suite of high-angle reverse faults within the central and southern parts of the Salar de Atacama Basin (Fig. 8F) (Jordan et al., 2002a,b). A secondary set of reverse faults at the eastern extreme of the Salar, with much less offset, uplifted the basin relative to the uplands to the east. The eastern sector of the Salar tilted approximately 0.5–2.5° to the west; we estimate this tilt by subtracting a correction of approximately 1.5° from the current dips, which accounts for both the primary depositional dip of the base of M (in most measured profiles likely $<0.5°$, given the lithologies of the K–M contact in the Toconao-1 borehole) and the maximum estimate of differential compaction of the underlying Cenozoic units to reduce their pre-M thicknesses by approximately 10%. This tilt represents rotation on the limb of a long-wavelength fold.

A separate late Miocene basin was active simultaneously SE of the Salar, where the Estratos de Quepe accumulated at least 700 m thickness (Fig. 5A). Blanco (unpublished data) reports an age of 9 Ma for a reworked ash layer in the Estratos de Quepe intercalated with volcanoclastic fluvial deposits derived from the southeast. This small subbasin may be characteristic of fault-bounded blocks east of the Salar; if that extrapolation is justified, other such basins remain buried beneath the Pliocene ignimbrites.

5.2. Sequence K/Paciencia Group

Kape (1996) reviews the likely age relations among the discontinuous surface outcrops of the Paciencia Group in the northern Cordillera de la Sal and flanking Llano de la Paciencia. Participation of upper Oligocene and lowest Miocene strata is confirmed by K/Ar and Ar/Ar dates on interbedded ashes, which range between 28 and 20 Ma (Travisany, 1979; Marinovic and Lahsen, 1984; Mpodozis et al., 2000). Kape (1996) also posits that the magnetic polarity reversal patterns in strata that lack datable ash interbeds represent older horizons, extending the age of the lower Paciencia Group sediments to 30 Ma.

In contrast, little record exists of the late–early to middle Miocene interval in exposures surrounding the Salar area, except for isolated flows associated with the small Cerro Jorquencal volcano (K/Ar biotite age: 17 ± 2 Ma, Ramírez, 1979), which unconformably overlie folded Paciencia Group sediments to the northeast of the Salar Basin. Along the northwestern flank of the drainage basin, inclusive of Cerros de Purilactis and the headwaters of the neighboring Calama Basin, Cowan et al. (2004) show that the middle Miocene is represented mostly by arid paleosols. In Llano de la Paciencia, similar paleosols are overprinted on the upper exposed surface of the Paciencia Group and overlain by late Miocene ignimbrites. The lack of Middle Miocene strata in exposures west and northwest of the modern Salar likely reflects, in part, a hyper-arid situation that deterred erosion and sediment transport. The only sedimentary

Table 1
Summary of evidence within basin of causes of accommodation

Sequence	Criteria				
	Contemporaneous faults and folds	Pattern of accumulation	Onlap/truncation patterns	Other	Interpretation of accommodation space
H Paleocene	None within basin nor any recognized growth strata; modest folding post-dates H	Thickness <3000 m; multiple short-wavelength depocenters	Onlaps folded top surface G; little erosional truncation of G		Largely post-deformational, filling basin formed by late Cretaceous and earliest Paleocene E–W shortening
J Eocene-early Oligocene	None within Salar; progressive unconformities in exposures to W suggest contractional structures in Cordillera Domeyko	Greatest thickness west of southern Salar; thickness in Salar <1000 m; thickness variations reflect deep erosion of top of J	Minimal onlap suggests low relief when J began to accumulate; H truncated below J		True tectonic subsidence only west of Salar; within Salar fill of topographic low remnant from earliest Paleocene after modification by pre-J regional tilt to east
K Oligocene-middle(?) Miocene (−30 to −10 Ma)	Near-vertical Paciencia Fault separates basin (east) from uplands (west); small normal faults near trace of Paciencia Fault offset Oligocene–Cretaceous unconformity and are in turn capped by Oligocene strata; early Miocene folds in CdlS[a] capped by 17 Ma lavas; Tulor reverse fault uplifts CdlS; initial diapirism & Salt withdrawal	Greatest thickness (>5000 m) along western margin; thickens monotonically westward from central axis of Salar; upper subsequence spatially Uniform except within 5 km of northern CdlS where it thickens	Onlap to east of top of J; several internal, gently angular unconformities	Oligocene–early Miocene evaporites in western sector of basin and siliciclastics in eastern sector of basin; middle Miocene an unconformity in outcrop; closed drainage basin	Normal fault (possibly transtensional) created >5000 m of accommodation, and relocated western border of Salar basin −10 km east of Paleocene border
M late Miocene–Quaternary (−10–0 Ma)	Unit K salt domes in CdlS grow synchronous with M; SFS near-vertical reverse offset −700 m in salar center but relief entirely masked by M halite accumulation; Peine Faults on eastern border cause uplift of basin relative to margin	<500 m in LIP[b]; >1000 m beneath most of Salar, with asymmetric thickening on east side SFS and northern CdlS	Conformable with top of K below most of Salar; onlaps salt dome (K) on east flank northern CdlS	Halite dominates 2500–3000 km^3; closed drainage basin; base of M dips ~2–4°W beneath eastern sector of Salar	Remnant accommodation still available from Oligocene; possible new accommodation generated by relative uplift of Andean slope to east by long-wavelength rotation; new faults create local accommodation space

[a] CdlS, Cordillera de la Sal.
[b] LIP, Llano de la Paciencia.

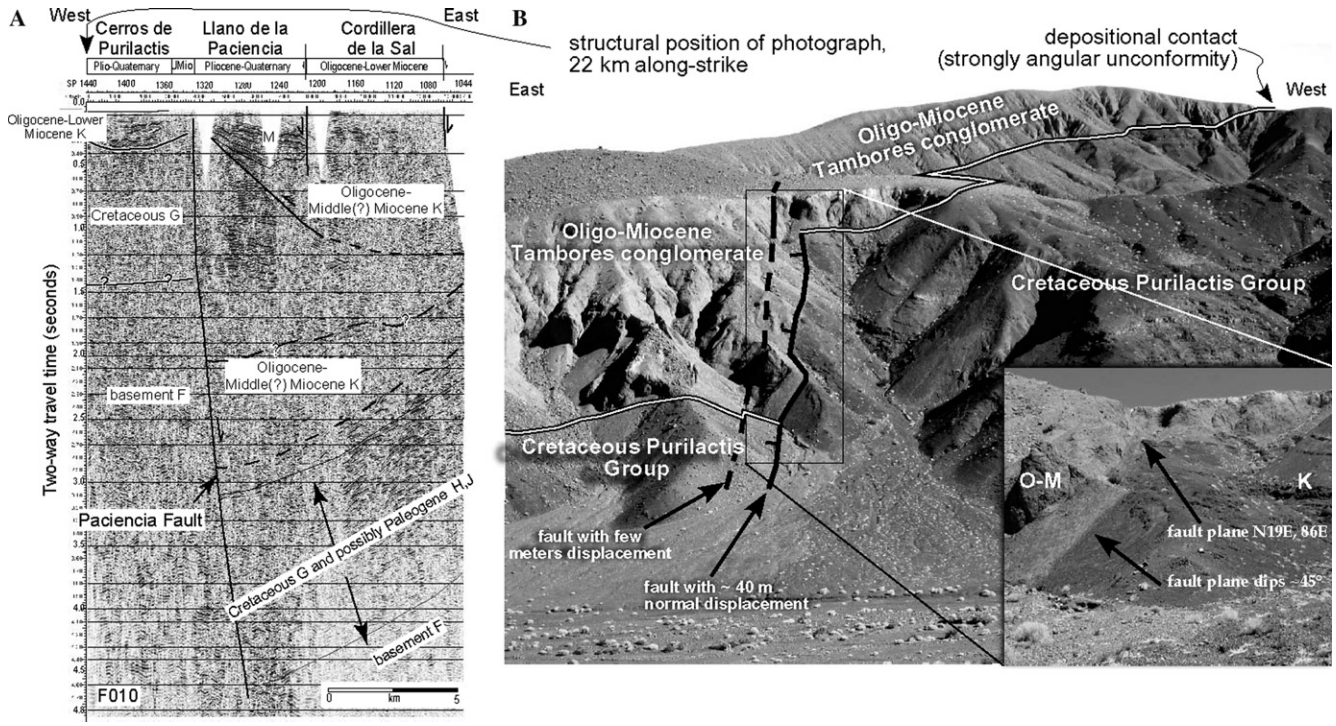

Fig. 7. Key relations at the western border of the Oligocene–Middle Miocene Salar de Atacama Basin, in which the Paciencia Group accumulated. Note that the view is to the north in (A) but to the south in (B). (A) Line F010 crosses the border between Cerros de Purilactis and the Oligocene and younger Salar de Atacama Basin (now Llano de la Paciencia and Cordillera de la Sal). The quality of the seismic data are poor, but together with neighboring seismic lines and surface geologic data, they reveal over 6(±1) km down-to-the-east apparent stratigraphic displacement and at least 3 km true vertical displacement across the Paciencia Fault and that the dip of the fault is near vertical (Pananont et al., 2004). (B) Photograph of relations along a secondary fault west of Pampa Vizcachita (see Fig. 2 for location). The contact between the Cretaceous Purilactis Group strata and Oligo–Miocene Tambores conglomerate is an angular unconformity, visible at a distance, which is displaced locally by a normal fault with several tens of meters of down-to-the-east displacement. In nearby exposures, this or a similar fault is overtopped depositionally by the Tambores conglomerate. These outcrop relations, located 4 km west of the major subsurface Paciencia fault, illustrate that normal faults of Oligocene or younger age border the eastern flank of the Cerros de Purilactis and parallel the Paciencia fault.

accumulations known in outcrop are the Hollingsworth gravels (Naranjo et al., 1994), which overlie the hyperarid paleosols (Cowan et al., 2004) and underlie a 10 Ma ignimbrite. Although the Hollingsworth gravels are spatially extensive in the eastern Cordillera Domeyko and Cerros de Purilactis, they are only 2 m thick.

In the same exposures treated by Kape (1996), Wilkes and Görler (1994) suggest that thickness changes in the basin during accumulation of the Paciencia Group indicate transpressional syndepositional faulting. Flint et al. (1993) state that minor, normal faulting occurred in southern sectors of the Llano de la Paciencia during this time. West of the trace of the Paciencia Fault, a thin strip of Paciencia Group strata crops out along the west flank of the Vizcachita valley (“V” in Figs. 2 and 5A), where the basal contact of the Paciencia Group is a gently east-dipping angular unconformity above strongly folded Purilactis Group strata. Locally, that contact is cut by at least one steep, east-facing normal fault with tens of meters of displacement, as well as by smaller-scale normal faults (Fig. 7B). Some

Fig. 8. Sequential cartoon cross-sections illustrating the evolution of the Salar de Atacama Basin since the deformation that occurred at approximately the Cretaceous–Paleocene boundary. The cross-section is a composite of features well constrained in the northwestern and southeastern Salar (see locations in Fig. 2). Strata in the same stratigraphic sequence as the age of the cross-section are highlighted in gray. (A) Paleocene sequence H fills the tectonic subsidence generated by earliest Paleocene reverse faulting and folding at the western margin of and within the Salar de Atacama Basin. (B) The unconformity between sequences H and J reflects eastward rotation of a region that was broader than the sequence H basin and the erosional beveling of sequence H. (C) Eocene sequence J represents sediment shed from tectonically active highlands located tens of kilometers west of the Salar de Atacama Basin, which filled remnant accommodation space. (D) Oligocene lower sequence K fills an extensional (or transtensional) basin, whose western boundary was a set of east-facing normal faults. (E) Minor thrusting within the western sector of the Salar de Atacama Basin initiates uplift of the Cordillera de la Sal and triggers local salt doming, as well as salt withdrawal from the areas adjacent to Cordillera de la Sal. The middle(?) Miocene part of sequence K fills remnant accommodation space that was modified by localized subsidence (both tectonic and salt-withdrawal) at the borders of Cordillera de la Sal. (F) Accommodation space for sequence M accumulation is controlled by a complex combination of local deformation and basinwide remnant accommodation. Salt withdrawal locally produces a large amount of subsidence adjacent to salt domes in Cordillera de la Sal. Note that the salt diapir formed late in sequence K time migrated up-dip to the west during unit M time, creating an overhang of K (exposed in the Cordillera de la Sal) over units H, J, and K. Large-offset reverse faults within the Salar (SFS, Salar fault system) produce footwall tectonic subsidence.

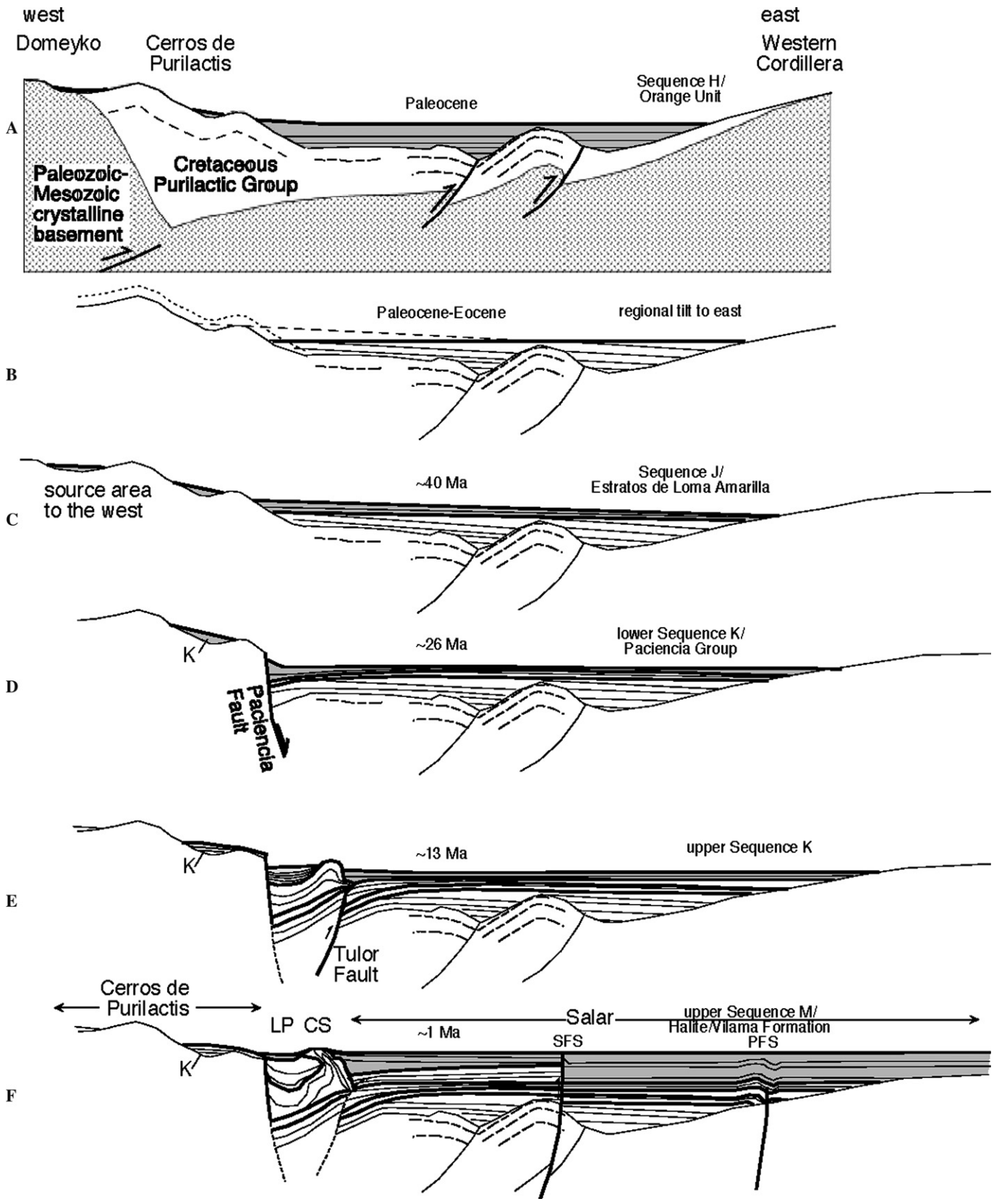
west
Domeyko
Cerros de Purilactis
east
Western Cordillera
A
Paleocene
Sequence H/ Orange Unit
Paleozoic-Mesozoic crystalline basement
Cretaceous Purilactic Group
B
Paleocene-Eocene
regional tilt to east
C
source area to the west
~40 Ma
Sequence J/ Estratos de Loma Amarilla
D
K
Paciencia Fault
~26 Ma
lower Sequence K/ Paciencia Group
E
K
~13 Ma
upper Sequence K
Tulor Fault
F
Cerros de Purilactis
LP CS
Salar
upper Sequence M/ Halite/Vilama Formation
~1 Ma
SFS
PFS
K

of those normal faults are overlapped and sealed by higher horizons in the Paciencia Group (Pananont et al., 2004). We posit that this part of the Paciencia Group Basin was a secondary half-graben in the upthrown block of the principal Paciencia fault. Although the dip of the major basin-bounding Paciencia fault is not clearly revealed by the seismic data, these surface relations cause us to interpret it as a steep normal fault (Fig. 8D). Although in similar locations relative to the regional-scale Paciencia fault, the Paciencia Group conglomerates well exposed in Quebrada Tambores ("QT" of Fig. 5C) likely accumulated in a topographic low (synclinal axis), a remnant of the latest Cretaceous folding of the Purilactis Group (Fig. 8D), whereas the Pampa Vizcachita subbasin was related to contemporaneous extensional (transtensional?) deformation.

Surface exposures of the Paciencia Group (San Pedro and Tambores formations) display marked facies variations between halite- and gypsum-dominated salar facies, coarse alluvial fan facies, and many intermediate depositional environments (Fig. 4). Despite the evidence that, in certain sections, these environments succeed one another transitionally (Flint, 1985; Jolley et al., 1990; Kape, 1996; Wilkes and Görler, 1994), unconformities within sequence K are clear beneath the Salar (Fig. 3). Thus, abrupt contacts between dissimilar facies (e.g., conglomerates over evaporite facies) like those reported by Mpodozis et al. (2000) near Pampa Vizcachita ("V" in Figs. 2, 5B; Camp 2 section of Kape, 1996), though not discernibly discordant, likely represent typical relations across the seismically defined high-order subsequence boundaries within the lower K subsequence and may represent hiatuses lasting hundreds of thousands to millions of years.

The unconformable relations between the Paciencia Group and the 17 Ma lavas from the Jorquencal volcano imply that the Northern Cordillera de la Sal was a region of shortening and a low ridgeline that grew during the early–middle Miocene (Fig. 8E). We believe that a significant part of the thousands of meters of upper sequence K strata in the Llano de la Paciencia (Fig. 7A) ponded behind the incipient uplifted ridge of Cordillera de la Sal.

Thicknesses of sequence K beneath the central and eastern Salar de Atacama (~1000 m) are considerably less than the 2000–3000 m thickness reported in the northern Cordillera de la Sal (Wilkes and Görler, 1994; Kape, 1996). Long-wavelength rotation to the west of the western 15 km of the Salar region is evident from the thickness patterns and onlap relations among subsequences within K (Figs. 3 and 5B). The 30 km width of the structural basin, from the trace of the western boundary normal fault(s) to a thickness minimum of the lower subsequence near the Salar center, is consistent with subsidence in an extensional half-graben (Leeder, 1995). Judging by the mudstone composition of sequence K in the Toconao-1 borehole, restriction of the evaporite facies to the western, proximal part of the basin is consistent with underfilling of the basin during stages of high rates of subsidence.

Without generating significant sedimentary basins, complex normal and reverse displacement associated with the time of unit K occurred near the eastern margin of the Salar de Atacama Basin. As shown in a seismic line (Fig. 6B) that captures the west flank of the only structural high that exposes pre-upper Miocene units, two zones of small offset faults displaced not only units H and J but also appear to have cut the lower part of sequence K. These faults coincide with some of the Cretaceous basin-bounding faults. Some splays experienced normal displacements on the order of hundreds of meters very early in unit K accumulation and moderate reverse displacement later during unit K accumulation. These complex and varying relationships across steep faults are typical of strike-slip fault systems (Nilsen and Sylvester, 1995).

In summary, a combination of factors contributed to the accommodation space for sequence K (Figs. 8D and E). During the Oligocene and early Miocene, normal faulting at the western border of the basin served as a dominant control. However, the persistence of many hundred of meters of the lower subsequence of K to the eastern sector of the Salar and continued onlap of the post-Purilactis Group erosional surface in that eastern region (Fig. 6A) suggest that sequence K also filled remnant space from the earliest Paleocene folding event. Thickness patterns of the upper subsequence reveal local changes in base level in response to uplift and salt diapirism along the Cordillera de la Sal but no additional, large magnitude tectonic displacement of the basin margins. Thus, we argue that many hundred meters thickness of upper sequence K filled remnant accommodation space created during the late Oligocene and the end of the Cretaceous.

5.3. Sequence J/Loma Amarilla Formation

The Eocene Loma Amarilla Formation/sequence J represents an interval of subdued local relief compared with the localized depocenters of sequence H. Comparison of the isopach maps of J and H (Figs. 5C and D) reveals both a longer wavelength of the depocenters and little correlation of sequence J depocenters with those of sequence H. In the center of the Salar, sequence J fills a topographic low generated by the tilt of its substrate to the east and limited eastward by a late Cretaceous, west-facing paleoslope (Figs. 6, 8B and C). At the surface, Loma Amarilla conglomerates consist of clasts of lithologies that must have been derived from the Cordillera de Domeyko the west of El Bordo Escarpment (Mpodozis et al., 2005). A western source area in the region strongly affected by Incaic deformation (Scheuber and Reutter, 1992; Mpodozis et al., 1993a; Maksaev and Zentilli, 1999) is consistent with the considerably thicker exposure of the Loma Amarilla Formation west of the Salar along the southern El Bordo escarpment compared with sequence J below the Salar (Fig. 5C) (Mpodozis et al., 2005). Especially in the southern part of the system, the western margin of the Eocene Salar de Atacama Basin did not coincide with

the Oligocene–early Miocene basin margin. No faults contemporaneous with sequence J have been identified in or adjacent to Salar de Atacama. We suggest that within the confines of the Salar Basin, sequence J accumulated largely because accommodation space remained from the earliest Paleocene deformation.

5.4. Sequence H/Orange Formation

The Orange Formation/sequence H filled a very irregular surface topography generated by earliest Paleocene compressional folding (Figs. 3 and 8A). Beneath much of the Salar and in exposures to the west, the folded strata include uppermost Cretaceous horizons, not much older than the Paleocene Orange Formation. Mpodozis et al. (1999, 2005) demonstrate that locally exposed units to the west provided the source of the Paleocene Orange Formation sediments. The western margins of the fold system and the Orange Formation coincide with the contact between a basement-cored fold (Paleozoic–Triassic basement) and the Cretaceous sedimentary sequences exposed along the El Bordo escarpment (Fig. 5D) (Arriagada et al., 2002). The Orange Formation/sequence H accumulated above a 60 km wide zone of extensive folding. Consequently, we posit that sequence H/Orange Formation followed compressional uplift of the pre-Cretaceous basement of the Cordillera de Domeyko and folding of the late Cretaceous Purilactis Group strata both at the eastern edge of the Cordillera de Domeyko and in the Salar de Atacama Basin domain to the east (Figs. 5D and 8A). This scenario could be characterized as deposition in a "wedge-top" position in the sense of DeCelles and Giles (1996), though knowledge of the nature of the faults that controlled the folds is insufficient to verify the existence of a wedge-like deformation zone.

5.5. Stratigraphic summary

In summary, the western margin of the Cenozoic Salar de Atacama Basin first was controlled by the Cordillera de Domeyko basement structural high, which limited a broad fold belt extending eastward below the basin (Fig. 8A). The western boundary was a basement-cored fold, interpreted as related to a blind, east-verging reverse fault, which began to grow during the structural inversion of the Jurassic–early Cretaceous Tarapacá backarc Basin (Mpodozis and Ramos, 1990; Mpodozis et al., 2005) and was reactivated by renewed compression in the earliest Paleocene. The boundary of sedimentary accumulation shifted to the west during the Eocene–earliest Oligocene Incaic deformation, probably to a position close to the axis of the Cordillera de Domeyko (Fig. 8C). During the Oligocene, the western basin boundary stepped eastward to a position largely controlled by the east-facing Paciencia normal fault (Fig. 8D) and became a pronounced basin divide again. Progressive erosion of the fault scarp, continued fill of remnant accommodation space (a local synclinal topographic low), and fault definition of a subsidiary basin led to localized westward overstep of the Paciencia normal fault during accumulation of the Paciencia Group. Although the western boundary of the Salar de Atacama Basin changed little during the Neogene, the growth of the intrabasinal Cordillera de la Sal, beginning in the latest early Miocene (Ramírez, 1979), subdivided the western part of the basin into two depocenters (Figs. 8E and F). The Oligocene–early Miocene normal fault served as the western boundary of the middle Miocene–Quaternary basin because the flow of Paciencia Group halite up-dip from its fault-controlled depocenter caused salt-withdrawal faulting (coincident in location but not tectonic origin with the Oligocene normal fault) and subsidence. Salt flow dominated deformation and subsidence patterns of the northern half of the basin region, but tectonically, activity is well expressed in the deformation and subsidence of the southern half of the basin.

This study does not resolve the process responsible for the El Bordo escarpment (Fig. 1) (Naranjo et al., 1994). This 150 km long, east-facing scarp defines the border of the modern Llano de la Paciencia drainage basin south of the Cerros de Purilactis. The relief between the escarpment and the Llano de la Paciencia is approximately 800 m. West of the divide, a gentle slope is covered by the uppermost middle–lowermost upper Miocene Hollingsworth gravels, whereas the eastern face is two to three times steeper and more deeply eroded. The escarpment parallels but lies 5–12 km to the west of the Paciencia fault. Data presented here do not reveal whether this scarp represents late Miocene–Quaternary tectonic subsidence of the western part of the Salar de Atacama Basin or is instead a progressive landscape adjustment to a relief created during the Oligocene and locally reshaped by progressive salt flow beneath the Llano de la Paciencia.

The modern eastern margin of the Salar de Atacama Basin corresponds to a prominent west-dipping slope, and the eastern terminations of Cenozoic strata onlap a prominent west-dipping unconformity. The angularity of the unconformity between Paleocene sequence H and Cretaceous sequence G implies that Cretaceous strata immediately east of the basin were folded during the earliest Paleocene (Fig. 8A). From the Paleocene through the end of the Miocene, erosion of the slope and fill of the basin led to progressively eastward sedimentary onlap of that structural slope (Figs. 8B–F). Finally, during sequence M/Vilama time (late Miocene–Recent), when sediment supply to the Salar was associated with the emplacement of major ignimbrite sheets of eastern provenance, the Salar de Atacama Basin strata broadly overstepped the latest Cretaceous–Paleocene basin border (Fig. 8F). Simultaneously, since approximately 10–5 Ma, the eastern part of the Salar rotated 0.5–2.5° west. The shallow subcrop of Paleozoic basement rocks as part of the eastern slope, largely hidden beneath Pliocene ignimbrites, and the major thickness of Cretaceous strata immediately to the west (Fig. 6B) suggest that the Cretaceous structural relief along

buried faults located east of the Salar may have been similar in magnitude to the structural relief across the east flank of the Cordillera Domeyko.

6. Basin evolution in relation to regional tectonics

We propose four different Cenozoic regional tectonic stages expressed by subsidence and fill of the Salar de Atacama Basin. The first, in the Paleocene, was a consequence of earliest Paleocene crustal shortening (Fig. 8A) in a backarc setting. The second was contemporaneous with the Eocene–early Oligocene Incaic deformation episode (Fig. 8C) associated with transpressional deformation, block rotations, and tectonic uplift in the Cordillera Domeyko, where fault-controlled shallow-level plutonism included the emplacement of giant porphyry-copper deposits like Chuquicamata and La Escondida (Fig. 1) (Mpodozis et al., 1993a; Scheuber et al., 1994; Maksaev and Zentilli, 1999; Arriagada et al., 2000; Tomlinson et al., 2001). The third relates to the enigmatic Oligocene and early Miocene times (Fig. 8D) characterized regionally by a magmatic lull. Finally, during the fourth and youngest tectonic state (Figs. 8E and F), the basin was located in the forearc of the Andean central volcanic zone.

The Paleocene Orange Formation/sequence H represents a late syndeformational to postdeformational step in the long-term filling of a major structural low initiated by late Cretaceous inversion of the Jurassic–early Cretaceous Tarapacá backarc Basin. During the late Cretaceous, the poorly layered late Paleozoic–Triassic volcanic and intrusive units, which dominate in Cordillera de Domeyko, were uplifted by shortening across reverse faults that verge both east and west and change direction with latitude (Tomlinson et al., 2001). Unfortunately, the eastern, northern, and southern extents of the late Cretaceous Salar de Atacama (Purilactis) Basin and its internal geometry are not yet well defined. Faults in the Salar de Atacama Basin region were reactivated during the earliest Paleocene (Arriagada, 2003; Mpodozis et al., 2005). Consequently, the Orange Formation/sequence H can be considered the largely postdeformational fill of a 60 km wide basin built on top of a rotational block in the footwall of a major blind reverse fault (Table 1, Fig. 8A).

The broader basin in which the Loma Amarilla conglomerates and sequence J accumulated was contemporaneous with and 40–50 km east of a belt of deformation in the Cordillera de Domeyko during the late Eocene–early Oligocene Incaic event (Maksaev, 1990; Mpodozis et al., 1993a,b; Marinovic and Garcia, 1999). Mapping and paleomagnetic rotation studies show that, at the latitude of the Salar de Atacama, the Incaic deformation was dominated by arc-parallel sinistral strike-slip faulting and clockwise rigid-body block rotations about vertical axes (Mpodozis et al., 1993a; Arriagada, 1999). Even though these styles of deformation do not necessarily cause major crustal thickening, Alpers and Brimhall (1988), Andriessen and Reutter (1994), and Maksaev and Zentilli (1999) show that almost 3–4 km of exhumation occurred west of the Salar de Atacama during the late Eocene–early Oligocene. Slightly farther north, near 21–23°S, only east-west-oriented shortening occurred during the Incaic event (Tomlinson and Blanco, 1997), and the Calama Formation accumulated in a proximal basin (Blanco et al., 2003).

To the northeast, in southern Bolivia, thousands of meters of nonmarine clastic strata accumulated rapidly during the late Eocene and Oligocene (Horton et al., 2001, 2002). Horton et al. (2001, 2002) consider that this broad late Paleogene basin was a foreland basin. Similarly, Jordan and Alonso (1987) speculate that the Eocene Geste Group strata of the Puna southeast of the Salar de Atacama Basin accumulated in a foreland basin. Muñoz et al. (1997) attribute the Eocene–Miocene sequences J and K to a flexural subsidence coupled with a compressional highland located to the west. However, in each case, the proposed "foreland basin" relationship between tectonic subsidence and the Eocene–early Oligocene Incaic deformation to the west rests only on general regional relations, not structural geologic evidence that a thrust belt mechanically coupled with a flexural basin existed. Considering all the data, we argue that Eocene deposition in the Salar de Atacama Basin resulted from sediment supply from a broadly uplifted transpressional highland, which accumulated in remnant accommodation space, slightly modified by regional tilt (Table 1, Fig. 8B and C).

The Oligocene–early Miocene time of the Paciencia Group and lower sequence K was regionally complex. Due either to the extensive cover of upper Miocene–Quaternary ignimbrites and stratovolcanoes (Ramírez and Gardeweg, 1982; Marinovic and Lahsen, 1984; De Silva, 1989a) or likely to the true absence of significant late Oligocene–early Miocene volcanic activity, at the latitudes of the Salar de Atacama, no evidence exists for a well-established, late Oligocene–early Miocene volcanic arc (Kay et al., 1999). The tectonic regime prevailing during this period is regionally unknown. To the northeast of the Salar de Atacama Basin, thrust deformation controlled the 28–20 Ma interval in the Southern Bolivian Eastern Cordillera (Horton, 1998; Horton et al., 2005), whereas in the southern Altiplano, it was a time of tectonic quiescence (Elger et al., 2005) or extension (Scheuber et al., 2005). In the Argentine Puna southeast of Salar de Atacama, though Kraemer et al. (1999) interpret the local accumulation of upper Oligocene coarse clastic strata as the product of local thrusting, their evidence indicates only that differential uplift and likely faulting existed; they fail to demonstrate the nature of the faults. Accumulation in the broad Calama Basin, which neighbors the Salar de Atacama Basin to the northwest (Fig. 1), was controlled by a set of major normal faults of the same age as the Paciencia fault (Jordan et al., 2004). Tomlinson et al. (2001) show that the contemporaneous but much smaller Papajoy Basin, located north of Calama Basin (Fig. 1), was an in-line graben formed within a strike-slip fault system (West Fissure Fault) responsible for 35 km of left-lateral displacement between 31 and 17 Ma.

New data (Pananont et al., 2004) show that the tectonic subsidence of the Oligocene–early Miocene Salar de Atacama Basin was due to east–west extension or transtension. Rapid thickness changes and complex facies relations within the Llano de la Paciencia and Cordillera de la Sal reflect their proximity to the faulted basin margin, whereas multiple unconformities and longer wavelength tilt of the western floor of the Salar reflect hangingwall rotation (Table 1, Fig. 8D). The steep dip (~80°) of the Paciencia fault would accommodate only a small magnitude of extension (Pananont et al., 2004). The data available in this study are insensitive to possible vertical axis strain, and thus, we cannot evaluate whether the east–west extension occurred within a transtensional strain field. However, the large magnitude of apparent stratigraphic displacement across a single normal fault exceeds values typical in extensional systems and may be more typical of transtensional systems (Leeder, 1995; Nilsen and Sylvester, 1995), in which horizontal displacement of tilted units contributes to apparent vertical stratigraphic offsets. On a small scale, the complex relations displayed by minor faults in the southeastern Salar (Fig. 6B) are also consistent with Oligo-Miocene strike-slip deformation.

Over a surface area of at least 12,000 km^2, located more than 200 km east of the contemporaneous trench axis, small-magnitude east–west extension was responsible for subsidence and relief generation in the two principal Oligocene–early Miocene sedimentary basins of northern Chile. The overall tectonic setting is not well understood, but apparently the Calama and Salar de Atacama basins are neither forearc nor backarc, as there was no contemporaneous arc of this time interval between 22° and 24°S. Kay et al. (1999) proposed that this segment of the Andes was underlain by a subducted plate with a subhorizontal trajectory at a shallow depth. However, even beyond this latitudinal belt, the tectonic state of the late Oligocene and early Miocene was transitional, associated with a major eastward leap in the position of the volcanic arc, and in the Southern Andes, widespread small-magnitude extension rather than shortening occurred (Jordan et al., 2001).

Since the middle Miocene, a normal continental margin arc system located east of the Salar de Atacama Basin has dominated the regional tectonic setting (Ramírez and Gardeweg, 1982; Kay et al., 1999), placing the basin in a forearc position while uppermost sequence K and sequence M accumulated. Accumulation of upper sequence K (Fig. 8E) represents a combination of a small degree of new tectonic subsidence along the eastern margin of the Cordillera de la Sal, fill of salt-withdrawal basins west of Cordillera de la Sal, and fill of a broad remnant topographic low without evidence (i.e., contemporaneous faults, highly asymmetric thicknesses of strata) of further tectonic subsidence.

Although we can readily explain controls on the late Miocene–Quaternary Salar de Atacama Basin (Fig. 8F) on a local scale, we do not yet understand their regional tectonic significance. Despite 3 km relief to the crests of volcanic centers east of the basin, a hyperarid climate suppressed erosion both east and west of the basin, as clearly indicated by the lack of major erosional dissection of the eastern slopes. Instead, the sediment volume is dominated by chemical sediment (halite) and ignimbrites. Jordan et al. (2002a,b) suggest that the halite is a product of deep groundwater flow driven by the elevation contrast across the western flank of the Altiplano-Puna plateau, and thus, the initiation of halite accumulation may be evidence of structural uplift of the Andean slopes east of the basin at approximately 5–10 Ma. The 0.5–2.5° rotation of the 5–10 Ma base of sequence M beneath the eastern Salar is consistent with that hypothesis and reflects the addition of accommodation space by long-wavelength rotation of the Andes (Table 1). This accommodation would be due to relative uplift of the basin margin rather than to tectonic subsidence. The sediments continued to fill the broad Atacama Basin topographic low (inherited and new accommodation space), while new sets of reverse faults (Salar and Peine fault systems) added local tectonic subsidence. The lack of spatial association of the new faults with major Cretaceous or older Cenozoic basin-bounding structures suggests that the controls on basin subsidence were much different than in earlier times. These new faults parallel faults exposed east of the Salar, such as the Miscanti reverse fault, along which several stratovolcanoes are located (Ramírez and Gardeweg, 1982). North of San Pedro, Hooper and Flint (1987) and Mpodozis et al. (2000) describe Plio-Quaternary thrusting on NNE-trending thrusts. A key component of the basin's regional setting is its location in what would have been the volcanic arc line, if the central volcanic zone did not swing approximately 100 km east of the shortest-distance path through the Salar (Fig. 1). We suggest that the Plio-Quaternary history of the Salar de Atacama Basin is tightly coupled with the features that either cause or accommodate the eastward deviation of the volcanic arc. Schurr and Rietbrock (2004) interpret that the eastward deflection of the magmatic arc is a consequence of an anomalous cold lithospheric block coincident with the Atacama Basin.

7. Conclusions

The entirely nonmarine Cenozoic Salar de Atacama Basin helps illuminate the nature of four distinct stages in the Cenozoic tectonic evolution of the Central Andes. During this period, the dominant regional tectonic mode was east–west shortening in a plate setting that involved varying degrees of margin-parallel strike-slip displacement. The most markedly different basin mode, in which subsidence was due to east–west extension during the Oligocene and early Miocene, may represent a significant change in plate interactions or a modest shift in a strike-slip-dominated system. Further regional kinematic study of Oligocene–early Miocene structures and basins of the western sector of the Central Andes are needed to clarify the strain field.

The late Cretaceous compressional inversion of the Mesozoic backarc basin system created both the major footprint of the Salar de Atacama Basin and the Cordillera de Domeyko as a north-trending basement high. Along the eastern margin of the Cordillera de Domeyko, the Purilactis Basin was trapped on the downthrown block and progressively more involved in folding. During the Paleocene, sequence H (Orange Formation) accumulated a set of more than 60 km wide folds in the Purilactis Group and was itself gently folded. A relatively long period of erosion followed, after which sediment shed from the Eocene–early Oligocene transpressional Incaic deformation, whose axis lay approximately 50 km west of the Salar de Atacama Basin, continued to fill the remnant basin as sequence J (Loma Amarilla Formation).

The development of a major down-to-the-east normal fault during the Oligocene moved the western basin margin approximately 10 km eastward compared with its early Paleocene position. Although tectonic subsidence created an excess of accommodation over sediment supply proximal to the fault, which encouraged accumulation of evaporites as well as siliciclastic strata, lower sequence K (Paciencia Group) strata also continued to fill the lowland remnant of the late Cretaceous–Paleocene subsidence. The extension-related halite of the western sector of the basin played a key role in the Miocene–Recent evolution of the basin, even though the tectonic environment returned to a compressional style. Progressive middle–late Miocene depositional infill of a landscape, which included structural ridges and basins produced by local offset of moderate magnitude reverse faults, caused differential burial of the Paciencia halite and triggered salt flow, which exaggerated the subdivision of the basin across the low ridge of Cordillera de la Sal. Although local tectonic subsidence along reverse faults generated complex variations within the Miocene to Recent basin, the long-wavelength controls on the basin pattern were the excess tectonic subsidence produced during the earliest Paleocene and Oligocene, which maintained the internal drainage of the basin, and relative uplift of the Andes east of the basin.

Acknowledgement

We sincerely thank ENAP/SIPETROL and SQM for access to their subsurface data, and FONDECYT grant 1990009 and NSF grant EAR-0208130 for financial support of this research. Discussions with our colleagues Linda Godfrey, Richard Allmendinger, Gregory Hoke, Larry Brown, Federico Dávila (Cornell), and Tim Lowenstein (Binghamton University) are appreciated. Reviews by Timothy Lawton and Brian Horton, which led to improvements in the manuscript, are gratefully acknowledged.

References

Alpers, C.N., Brimhall, G.H., 1988. Middle Miocene climatic change in the Atacama Desert, northern Chile; evidence from supergene mineralization at La Escondida. Geological Society of America Bulletin 100, 1640–1656.

Andriessen, P.A.M., Reutter, K.-J., 1994. K-Ar and fission track mineral age determination of igneous rocks related to multiple arc systems along the 23°S latitude of Chile and NW Argentina. In: Reutter, K.-J., Scheuber, E., Wigger, P.J. (Eds.), Tectonics of the Southern Central Andes, Structure and Evolution of an Active Continental Margin. Springer-Verlag, Berlin, pp. 141–153.

Arriagada, C., 1999. Geología y paleomagnetismo del borde oriental de la Cordillera de Domeyko entre los 22°45′ y 23°30′ latitud sur, II Región, Chile (MS. thesis). Universidad de Chile, Santiago, 176pp.

Arriagada, C., 2003. Rotaciones tectónicas y deformación del antearco en los Andes Centrales durante el Cenozoico (PhD thesis). Université de Rennes, France, and Universidad de Chile, Santiago, Chile, 308pp.

Arriagada, C., Roperch, P., Mpodozis, C., 2000. Clockwise block rotations along the eastern border of the Cordillera de Domeyko, northern Chile. Tectonophysics 326, 153–171.

Arriagada, C., Cobbold, P., Mpodozis, C., Roperch, P., 2002. Cretaceous to Paleogene compressional tectonics during deposition of the Purilactis Group, Salar de Atacama. Fifth International Symposium on Andean Geodynamics, Institute de Recherche pour le Développement, Paris, and Université Paul Sabatier, Toulouse, France, pp. 41–44.

Bevacqua, P., 1991. Geomorfología del Salar de Atacama y estratigrafia de su nucleo y delta, Segunda Región de Antofagasta, Chile (MS thesis). Universidad Católica del Norte, Antofagasta, Chile, 284pp.

Blanco, N., Mpodozis, C., Gardeweg, M., Jordan, T., 2000. Sedimentación del Mioceno superior-Plioceno en la Cuenca del Salar de Atacama: estratigrafía de la Formación Vilama, II Región de Antofagasta. IX Congreso Geológico Chileno 2, 446–450.

Blanco, N., Tomlinson, A.J., Mpodozis, C., Pérez de Arce, C., Matthews, S., 2003. Formación Calama, Eoceno, II Región de Antofagasta, Chile:estratigrafía e implicancías tectónicas. X Congreso Geológico Chileno, Universidad de Concepción, Chile (electronic paper, 10pp.).

Bobst, A.L., Lowenstein, T.K., Jordan, T.E., Godfrey, L.V., Hein, M.C., Ku, T.L., Luo, S., 2001. A 106 ka paleoclimate record from the Salar de Atacama, northern Chile. Palaeogeography, Palaeoclimatology, Palaeoecology 173, 21–42.

Cowan, A.M., Rech, J.A., Currie, B.S., 2004. Mid-Miocene hyperaridity in the Atacama Desert, Chile: evidence from the gypsic Barros Arana paleosol. Abstracts with program – Geological Society of America 36, 293.

Cross, T.A., Lessenger, M., 1988. Seismic stratigraphy. Annual Reviews Earth and Planetary Science 16, 319–354.

DeCelles, P.G., Giles, K.A., 1996. Foreland basin systems. Basin Research 8, 105–123.

De Silva, S.L., 1989a. Altiplano-Puna volcanic complex of the central Andes. Geology 17, 1102–1106.

De Silva, S.L., 1989b. Geochronology and stratigraphy of the ignimbrites from the 21°30′S to 23°30′S portion of the Central Andes of northern Chile. Journal Volcanology and Geothermal Research 37, 93–131.

Elger, K., Oncken, O., Glodny, J., 2005. Plateau-style accumulation of deformation: Southern Altiplano. Tectonics 24, TC4020, doi:10.1029/2004TC001675.

Flint, S., 1985. Alluvial fan and playa sedimentation in an Andean arid closed basin: the Pacencia Group, Antofagasta Province, Chile. Journal of the Geological Society of London 142, 533–546.

Flint, S., Turner, P., Jolley, E.J., Hartley, A.J., 1993. Extensional tectonics in convergent margin basins: an example from the Salar de Atacama, Chilean Andes. Geological Society of America Bulletin 105, 603–617.

Gardeweg, M., Ramirez, C.F., 1982. Geología de los volcanes del Callejón de Tilocalar, Cordillera de los Andes – Antofagasta. III Congreso Geológico Chileno, A111–A123.

Gardeweg, M., Ramírez, C.F., 1987. La Pacana caldera and the Atana Ignimbrite – a major ash-flow and resurgent caldera complex in the Andes of northern Chile. Bulletin of Volcanology 49, 547–566.

Gardeweg, M., Pino, H., Ramírez, C F., Davidson, J., 1994. Mapa geológico del area de Imilac y Sierra Almeida, Región de Antofagasta.

Servicio Nacional de Geología y Minería, Santiago, Chile, Documentos de Trabajo, 7 (1:100,000).

Hammerschmidt, K., Doebel, R., Friedrichsen, H., 1992. Implication of 40Ar/39Ar dating of early Tertiary volcanic rocks from the North-Chilean Precordillera. Tectonophysics 202, 55–58.

Hooper, B., Flint, S., 1987. Miocene – Recent tectonic evolution of the San Bartolo area, northern Chile. Zbl. Geol. Palaont 7/8, 967–981.

Horton, B.K., 1998. Sediment accumulation on top of the Andean orogenic wedge; Oligocene to late Miocene basins of the Eastern Cordillera, Southern Bolivia. Geological Society of America Bulletin 110, 1174–1192.

Horton, B.K., Hampton, B.A., Waanders, G., 2001. Paleogene synorogenic deposits in the Altiplano plateau and implications for initial mountain building in the central Andes. Geological Society of America Bulletin 113, 1387–1400.

Horton, B.K., Hampton, B.A., LaReau, B.N., Baldellón, E., 2002. Tertiary provenance history of the northern and central Altiplano (central Andes, Bolivia): a detrital record of plateau-margin tectonics. Journal of Sedimentary Research 72, 711–726.

Horton, B.K., 2005. Revised deformation history of the central Andes: inferences from Cenozoic foredeep and intermontane basins of the Eastern Cordillera, Bolivia. Tectonics 24, TC3011, doi:10.1029/2003TC001619.

Jolley, E.J., Turner, P., Williams, G.D., Hartley, A.J., Flint, S., 1990. Sedimentological response of an alluvial fan system to Neogene thrust tectonics, Atacama Desert, northern Chile. Journal of the Geological Society of London 147, 769–784.

Jordan, T.E., Alonso, R.N., 1987. Cenozoic stratigraphy and basin tectonics of the Andes Mountain, 20–28° south latitude. AAPG Bulletin 71, 49–64.

Jordan, T.E., Burns, W.M., Veiga, R., Pángaro, F., Copeland, P., Kelley, S., Mpodozis, C., 2001. Extension and basin formation in the Southern Andes caused by increased convergence rate: a mid-Cenozoic trigger for the Andes. Tectonics 20, 308–324.

Jordan, T.E., Godfrey, L.V., Muñoz, N., Alonso, R.N., Lowenstein, T.L. Hoke, G., Peranginangin, N., Isacks, B.L., Cathles, L., 2002a. Orogenic-scale ground water circulation in the Central Andes: evidence and consequences. In: 5th ISAG (International Symposium on Andean Geodynamics), Toulouse, France, Institut de Recherche pour le Développement, and Université Paul Sabatier, pp. 331–334.

Jordan, T.E., Muñoz, N., Hein, M., Lowenstein, T., Godfrey, L., Yu, J., 2002b. Active faulting and folding without topographic expression in an evaporite basin, Chile. Geological Society of America Bulletin 114, 1406–1421.

Jordan, T.E., Mpodozis, C., Blanco, N., Pananont, P., Dávila, F., 2004. Extensional basins in a convergent margin: Oligocene-early Miocene Salar de Atacama and Calama basins, Central Andes. Eos Transactions AGU 85 (47) Fall Meeting Supplement, Abstract T53A-0475.

Kape, S.J., 1996. Basin Analysis of the Oligo-Miocene Salar de Atacama, Northern Chile (PhD Thesis). University of Birmingham, Great Britain, pp. 1–256.

Kay, S.M., Mpodozis, C., Coira, B., 1999. Neogene magmatism, tectonism, and mineral deposits of the Central Andes (22° to 33°S latitude). In: Skinner, B.J. (Ed.), Geology and Ore Deposits of the Central Andes, Special Publication. 7 of Society of Economic Geologists, pp. 27–59.

Kraemer, B., Adelmann, D., Alten, M., Schnurr, W., Erpenstein, K., Kiefer, E., van den Bogaard, P., Görler, K., 1999. Incorporation of the Paleogene foreland into the Neogene Puna plateau: the Salar de Antofalla area, NW Argentina. Journal of South American Earth Sciences 12, 157–182.

Kuhn, D., 1997. Deformations analyse der Salar de Atacama region (Nordchile) und interpretation des neotektonischen Spannungsfelds (PhD thesis). Technical University, Berlin, Germany.

Leeder, M.R., 1995. Continental rifts and proto-oceanic rift troughs. In: Busby, C.J., Ingersoll, R.V. (Eds.), Tectonics of Sedimentary Basins. Blackwell Science, Oxford, pp. 119–148.

Lindsay, J.M., de Silva, S., Trumbull, R., Emmermann, R., Wemmer, K., 2001. La Pacana caldera, n. Chile: a reevaluation of the stratigraphy and volcanology of one of the world's largest resurgent calderas. Journal of Volcanology and Geothermal Research 106, 145–173.

Lowenstein, T.K., Hein, M.C., Bobst, A.L., Jordan, T.E., Ku, T.-L., Luo, S., 2003. An assessment of stratigraphic completeness in climate-sensitive closed-basin lake sediments: Salar de Atacama, Chile. Journal of Sedimentary Research 73, 91–104.

Macellari, C.E., Su, M.J., Townsend, F., 1991. Structure and seismic stratigraphy of the Atacama Basin, Northern Chile. VI Congreso Geológico Chileno, 133–137.

Maksaev, V., 1990. Metallogeny, geological evolution, and thermochronology of the Chilean Andes between latitudes 21 degrees and 26 degrees south, and the origin of major porphyry copper deposits (PhD thesis). Dalhousie University, Halifax, Canada, 554pp.

Maksaev, V., Zentilli, M., 1999. Fission track thermochronology of the Domeyko Cordillera, northern Chile: implications for Andean tectonics and porphyry copper metallogenesis. Exploration Mining Geology 8, 65–89.

Marinovic, S.N., Garcia, M., 1999. Hoja Pampa Unión. Región de Antofagasta. Servicio Nacional de Geología y Minería, Mapas Geológicos 9 (1:100,000).

Marinovic, S.N., Lahsen, A.A., 1984. Hoja Calama, Región de Atacama. Carta Geológica de Chile, Servicio Nacional de Geología y Minería 58, 140, plus map (1:250,000).

Mpodozis, C., Arriagada, C., Roperch, P., 1999. Cretaceous to Paleogene geology of the Salar de Atacama basin, northern Chile: a reappraisal of the Purilactis Group stratigraphy. In: Fourth International Symposium on Andean Geodynamics, Goettingen (Germany), pp. 523–527.

Mpodozis, C., Arriagada, C., Basso, M., Roperch, P., Cobbold, P., Reich, M., 2005. Late Mesozoic to Paleogene stratigraphy of the Salar de Atacama Basin, Antofagasta, northern Chile: implications for the tectonic evolution of the Central Andes. Tectonophysics 399, 125–154.

Mpodozis, C., Blanco, N., Jordan, T.E., Gardeweg, M.C., 2000. Estratigrafía, eventos tectónicos y deformación del Cenozoico tardío en la región norte de la cuenca del Salar de Atacama: la zona de Vilama-Pampa Vizcachita. IX Congreso Geológico Chileno 2, 598–603.

Mpodozis, C., Marinovic, N., Smoje, I., 1993a. Eocene left lateral strike slip faulting and clockwise block rotations in the Cordillera de Domeyko, west of the Salar de Atacama, northern Chile. In: International Symposium on Andean Geodynamics (ISAG), Oxford, UK, Editions de l'Office de la Recherche Scientifique et Technique d'Outre-mer (ORSTOM), France, pp. 225–228.

Mpodozis, C., Marinovic, N., Smoje, I., Cuitiño, L., 1993b. Estudio geológico-estructural de la Cordillera de Domeyko entre Sierra Limón Verde y Sierra Mariposas, Región de Antofagasta. Servicio Nacional de Geología y Minería, Informe Registrado IR-93-04, 1–282.

Mpodozis, C., Ramos, V.A., 1990. The Andes of Chile and Argentina. In: Ericksen, G.E., Pinochet, M.T.C., Reinemund, J.A. (Eds.), Geology of the Andes and its Relation to Hydrocarbon and Mineral Resources. In: Earth Science Series. Circum-Pacific Council for Energy and Mineral Resources. pp. 59–90.

Muñoz, N., Charrier, G.R., Jordan, T.E., 2002. Interactions between basement and cover during the evolution of the Salar de Atacama Basin, northern Chile. Revista Geológica de Chile 29, 55–80.

Muñoz, N., Charrier, R., Radic, J.P., 2000. Formación de la Cordillera de la Sal por propagación de fallas y plegamiento por despegue, II Región, Chile. IX Congreso Geológico Chileno 2, 604–608.

Muñoz, N., Charrier, G.R., Reutter, K.J., 1997. Evolución de la cuenca Salar de Atacama: inversión tectónica y relleno de una cuenca de antepaís de retroarco. VIII Congreso Geológico Chileno 1, 195–199.

Muñoz, N., Townsend, G.F., 1997. Estratigrafía de la cuenca Salar de Atacama. Resultados del pozo exploratorio Toconao-1, Implicancias regionales. VIII Congreso Geológico Chileno 1, 555–558.

Naranjo, J.A., Ramírez, C., Paskoff, R., 1994. Morphostratigraphic evolution of the northwestern margin of the Salar de Atacama basin (23°S-68°W). Revista Geológica de Chile 21, 91–103.

Nilsen, T.H., Sylvester, A.G., 1995. Strike-slip basins. In: Busby, C.J., Ingersoll, R.V. (Eds.), Tectonics of Sedimentary Basins. Blackwell Science, Oxford, pp. 425–458.

Pananont, P., 2003. Tectonic evolution of the northwest Salar de Atacama basin and northern Cordillera de la Sal, northern Chile: in Structure and tectonics of the Lunpola basin, Tibet, and the Salar de Atacama basin, northern Chile, and complications of deep AVO analysis. Ph.D. thesis, Cornell University, USA, pp. 58–140.

Pananont, P., Mpodozis, C., Blanco, N., Jordan, T.E., and Brown, L.D., 2004, Tectonic Evolution of the Northwest Salar de Atacama Basin, Northern Chile: Tectonics, TC6007, 10.1029/2003TC001595.

Ramírez, C.F., 1979. Geología del Cuadrángulo Río Grande y sector nororiental del Cuadrángulo Barros Arana, Provincia El Loa, II región. Memoria de título, Departamento de Geología, Universidad de Chile, Santiago, 139pp.

Ramírez, C., Gardeweg, M., 1982. Hoja Toconao, Región de Antofagasta. Servicio Nacional de Geología y Minería, Carta Geológica de Chile 54, 122, plus map (1:250,000).

Scheuber, E., Reutter, K.-J., 1992. Magmatic arc tectonics in the central Andes between 21° and 25°S. Tectonophysics 205, 127–140.

Scheuber, E., Bogdanic, C.T., Jensen, A.I., Reutter, K.-J., 1994. Tectonic development of the North Chilean Andes in relation to plate convergence and magmatism since the Jurassic. In: Reutter, K.J., Scheuber, E., Wigger, P.J. (Eds.), Tectonics of the Southern Central Andes; Structure and Evolution of an Active Continental Margin. Springer-Verlag, Berlin, pp. 121–139.

Scheuber, E., Mertmann, D., Ege, H., Silva-Gonzalez, P., Heubeck, C., Reutter, K.-J., Jacobshagen, V., (in press, 2005). Exhumation and basin development related to formation of the central Andean plateau, 21°S. In: Oncken et al., (Eds.), The Andes from top to bottom. Frontiers in Earth Sciences 1.

Schurr, B., Rietbrock, A., 2004. Deep seismic structure of the Atacama basin, northern Chile. Geophysical Research Letters 31, L12601. doi:10.1029/2004GL019796.

Tomlinson, A.J., Blanco, N., 1997. Structural evolution and displacement history of the West Fault system, Precordillera Chile: Part 1, Synmineral history. VIII Congreso Geológico Chileno, Antofagasta, Chile 3, 1873–1877.

Tomlinson, A.J., Blanco, N., Maksaev, V., Dilles, J.H., Grunder, A.L. Ladino, M., 2001. Geología de la precordillera andina de Quebrada Blanca – Chuquicamata, Regiones I y II (20°30′–22°30′ S). Servicio Nacional de Geología y Minería (Chile), Informe registrado IR-01-20, 2, 444 pp., 20 maps (1:50,000).

Travisany, A.V., 1979. Consideraciones geneticas sobre el yacimiento estratiforme San Bartolo. II Congreso Geológico Chileno 2, C149–C159.

Wilkes, E., Görler, K., 1994. Sedimentary and Structural Evolution of the Salar de Atacama, Northern Chile. In: Wigger, P., Reutter, K.J. (Eds.), Tectonics of the Southern Central Andes, pp. 171–188.